Development of end-to-end test phantom for stereotactic radiosurgery using alanine dosimeter

Miss Aungsumalin Intang

A Dissertation Submitted in Partial Fulfillment of the Requirements

for the Degree of Doctor of Philosophy in Medical Physics

Department of Radiology

FACULTY OF MEDICINE

Chulalongkorn University

Academic Year 2022

การพัฒนาหุ่นจำลองในการทดสอบแบบเอ็นทูเอ็น สำหรับรังสีศัลยกรรมร่วมพิกัดโดยใช้เครื่องวัดรังสีชนิดอะลานีน

น.ส.อังศุมาลิน อินแตง

| | |
|---|---|
| Thesis Title | Development of end-to-end test phantom for stereotactic radiosurgery using alanine dosimeter |
| By | Miss Aungsumalin Intang |
| Field of Study | Medical Physics |
| Thesis Advisor | Sornjarod Oonsiri, Ph.D. |

Accepted by the FACULTY OF MEDICINE, Chulalongkorn University in Partial Fulfillment of the Requirement for the Doctor of Philosophy

........................................................... Dean of the FACULTY OF MEDICINE

(Associate Professor CHANCHAI SITTIPUNT, M.D.)

DISSERTATION COMMITTEE

........................................................... Chairman

(Puangpen Tungboonduangjit, Ph.D.)

........................................................... Thesis Advisor

(Sornjarod Oonsiri, Ph.D.)

........................................................... Examiner

(Assistant Professor TAWEAP SANGHANGTHUM, Ph.D.)

........................................................... Examiner

(Assistant Professor Phannee Saengkaew, Ph.D.)

........................................................... External Examiner

(Assistant Professor Poramed Wongjom, Ph.D.)

อังศุมาลิน อินแตง : การพัฒนาหุ่นจำลองในการทดสอบแบบเอ็นทูเอ็น สำหรับรังสีศัลยกรรมร่วมพิกัดโดยใช้เครื่องวัดรังสีชนิดอะ
ลานีน. ( Development of end-to-end test phantom for stereotactic radiosurgery using alanine dosimeter) อ.ที่
ปรึกษาหลัก : อ. ดร.สรจรส อุณห์ศิริ

โดยทั่วไปแล้วเครื่องวัดปริมาณชนิดอะลานีนจะใช้ในการวัดปริมาณรังสีระดับสูง ซึ่งรังสีศัลยกรรมร่วมพิกัดใช้การฉายรังสีปริมาณ
สูงในครั้งเดียว จึงต้องมีระบบตรวจสอบตำแหน่งก่อนและระหว่างการฉายรังสีที่ช่วยให้การรักษามีความแม่นยำและถูกต้อง ดังนั้นจึงต้องมีการ
ทดสอบแบบเอ็นทูเอ็น ยิ่งไปกว่านั้นประเทศไทยยังไม่มีการทดสอบแบบเอ็นทูเอ็น สำหรับรังสีศัลยกรรมร่วมพิกัดโดยใช้เครื่องวัดรังสีชนิดอะ
ลานีน วัตถุประสงค์ของการงานวิจัยนี้เพื่อหาความถูกต้องของปริมาณรังสีในการรักษาด้วยวิธีรังสีศัลยกรรมร่วมพิกัดบริเวณสมองด้วยเทคนิคการ
ฉายรังสีปรับความเข้มโดยใช้หุ่นจำลอง วิธีการศึกษาเริ่มจากหาพารามิเตอร์ที่เหมาะสมของอิเล็กตรอนพาราแมกเนติกเรโซแนนซ์ (EPR) ในช่วง
ปริมาณรังสี 1-2000 เซนติเกรย์ แล้วนำพารามิเตอร์ที่ได้ไปศึกษาคุณสมบัติของอะลานีนพร้อมประเมินค่าความไม่แน่นอนสำหรับงานรังสีรักษา
หลังจากนั้นตรวจสอบความถูกต้องของปริมาณรังสี 1000 เซนติเกรย์ ที่พลังงาน 6 เมกะโวลต์แบบไม่ใช้แผ่นกรองลำรังสี ด้วยเครื่องวัดรังสี
ชนิดอะลานีน ณ หน่วยงานรังสีรักษา 8 หน่วยงานในประเทศไทย ขั้นตอนสุดท้ายออกแบบและประดิษฐ์หุ่นจำลองสำหรับหัว แล้วนำหุ่นจำลอง
นี้ไปตรวจสอบความถูกต้องของปริมาณรังสีโดยใช้เครื่องวัดรังสีชนิดอะลานีน ผลการทดลองพบว่า พารามิเตอร์ของอิเล็กตรอนพาราแมกเนติกเร
โซแนนซ์ (EPR) ที่เหมาะสมที่สุด ได้แก่ กำลังไมโครเวฟ(MP) แอมพลิจูด (MA) และคงที่ของเวลา (TC) มีค่าเท่ากับ 2 เมกะวัตต์ 7.018 เกาส์
และ 40.96 มิลลิวินาที ตามลำดับ โดยมีค่าความไม่แน่นอนแบบขยายของเครื่องวัดปริมาณรังสีชนิดอะลานีน 2.2 เปอร์เซ็นต์ ที่ระดับความ
เชื่อมั่น 95% (k=2) ในช่วงปริมาณรังสี 100-2000 เซนติเกรย์ ส่วนคุณลักษณะของเครื่องวัดรังสีชนิดอะลานีนที่พลังงาน 6 เมกะโวลต์แบบไม่ใช้
แผ่นกรองลำรังสีมีความสม่ำเสมอและมีความสามารถในการทำซ้ำได้ ซึ่งร้อยละของความแปรปรวนมีค่า 0.61 และ 0.22 ตามลำดับ ปริมาณของ
พาราแมกเนติกเรโซแนนซ์ (EPR intensity) เป็นสัดส่วนโดยตรงแบบเชิงเส้นกับปริมาณรังสีที่ฉาย ในช่วง 0-3000 เซนติเกรย์ (R$^2$ = 0.9998)
และสำหรับการทวนซ้ำได้ การขึ้นกับพลังงานและทิศทาง พบว่ามีค่า 0.80%, 0.80% และ 0.30% ตามลำดับ นอกจากนี้ ค่าการซีดจางใน
ระยะเวลา 3 เดือน มีค่าเท่ากับ 0.98% สำหรับหน่วยงานรังสีรักษา 8 หน่วยงานของเครื่องเร่งอนุภาค 9 เครื่อง ที่ทำการฉายเอาท์พุท 1000
เซนติเกรย์ พบว่าค่าร้อยละความแตกต่างไม่เกิน ±1% สำหรับหุ่นจำลองแบบใช้ไนลอนหล่อพบว่ามีค่าซีที ประมาณ 80-100 HU ซึ่งเป็นค่าที่
ใกล้เคียงกับเนื้อเยื่ออ่อน นอกจากนี้หุ่นจำลองแบบไนลอนหล่อมีราคาย่อมเยาว์กว่าหุ่นจำลองแบบเชิงพาณิชย์ สำหรับผลการทดลองฉายรังสี
ให้กับหุ่นจำลองแบบไนลอนหล่อ ด้วยวิธีรังสีศัลยกรรมร่วมพิกัดบริเวณสมองด้วยเทคนิคการฉายรังสีปรับความเข้ม พบว่าในก้อนมะเร็งมีร้อยละ
ความแตกต่างอยู่ระหว่าง 0.01 ถึง 1.16% แต่ในขณะที่ร้อยละความแตกต่างในก้านสมองมีค่ากว้างมากกว่า ตั้งแต่ 3.65 ถึง 11.95% ซึ่งใน
ตำแหน่งที่ 3 มีการผันแปรของปริมาณรังสีที่ก้านสมองมาก ในแผนการรักษา พบว่ามีค่าเบี่ยงเบนมาตรฐาน 19.7 17.8 และ 21.5 ในแผนการ
รักษา 1 2 และ 3 ตามลำดับ ส่งผลให้ปริมาณรังสีต่ำที่ก้านสมองมีความแตกต่างของปริมาณรังสีในก้านสมองมาก โดยสรุป หุ่นจำลองที่ใช้
ไนลอนหล่อ สำหรับใช้ในการทดสอบแบบเอ็นทูเอ็น สำหรับรังสีศัลยกรรมร่วมพิกัดโดยใช้เครื่องวัดรังสีชนิดอะลานีน มีการออกแบบที่เหมาะสม
โดยวัสดุชนิดไนล่อนหล่อมีความเหมาะสม สำหรับการใช้ในงานการฉายรังสีแบบรังสีศัลยกรรมร่วมพิกัด ในการทดสอบแบบเอ็นทูเอ็น โดยใช้
เครื่องวัดรังสีชนิดอะลานีน

| สาขาวิชา | ฟิสิกส์การแพทย์ | ลายมือชื่อนิสิต ................................................ |
|---|---|---|
| ปีการศึกษา | 2565 | ลายมือชื่อ อ.ที่ปรึกษาหลัก ............................ |

# # 6271036030 : MAJOR MEDICAL PHYSICS

KEYWORD:    End-to-end test, Head phantom, SRS, Alanine dosimeter, VMAT

Aungsumalin Intang : Development of end-to-end test phantom for stereotactic radiosurgery using alanine dosimeter. Advisor: Sornjarod Oonsiri, Ph.D.

Alanine dosimeters are generally used in high-dose dosimetry, while accurate and precise dose delivery verification procedures are important in stereotactic radiosurgery (SRS). Hence, an end-to-end test is required. In addition, no end-to-end SRS test employing an alanine dosimeter has been established in Thailand. The objective of this study was to determine the dose accuracy of SRS VMAT plans in end-to-end test phantom using alanine dosimeter. The electron paramagnetic resonance (EPR) parameters were optimized in the 1-2000 cGy dose range. Following that, suitable parameters were used to investigate the alanine characteristics and estimate the uncertainty in radiation therapy dose range. The alanine dosimeter system was then validated for output measurements in eight radiotherapy centers in Thailand at 1000 cGy at 6MV-FFF energy. Finally, a head phantom was fabricated and validated using an alanine dosimeter for end-to-end test in SRS. The optimized EPR parameters are microwave power of 2 mW, modulation amplitude of 7.018 G, and time constant of 40.96 ms. The expanded uncertainty (k=2) was 2.2% in the 100-2000 cGy dose range. The uniformity and reproducibility of the alanine dosimeter was studied in 6MV-FFF, with the percentage of CV being 0.61 and 0.22, respectively. The EPR Intensity demonstrated a linear proportion to the dose from 0 to 3000 cGy ($R^2$ = 0.9998). The repetition rate response, energy dependence, and directional dependence were 0.80%, 0.80%, and 0.30%, respectively. Furthermore, the fading in three months was 0.98%. The output survey in nine machine radiotherapy facilities was accurate to within ±1%. The phantom was made of cast nylon since it has a CT number of about 80-100 HU, which is close to soft tissue and is also a more commercially priced phantom. Volumetric modulated arc therapy (VMAT) SRS plans target percentage dose differences were ranging from 0.01% to 1.16%, while the percentage dose difference in the brain stem (OAR) ranged from 3.65% to 11.95%. A high variation of dose was found in Position 3 of TPS were SD=19.7, 17.8 and 21.5 in plan 1, plan 2 and plan 3, respectively. This contributes to a large dose difference when low dose at brainstem were performed. In conclusion, this study presented the fabricated cast nylon end-to-end test head phantom suitably designed to image and irradiate during an end-to-end test for stereotactic radiosurgery using alanine dosimeter.

| Field of Study: | Medical Physics | Student's Signature ............................. |
|---|---|---|
| Academic Year: | 2022 | Advisor's Signature ............................. |

# ACKNOWLEDGEMENTS

# TABLE OF CONTENTS

# LIST OF TABLES

# LIST OF FIGURES

## LIST OF ABBREVIATIONS AND SYMBOLS

| | |
|---|---|
| AAA | Analytical anisotropic algorithm |
| CNC | Computer numerically controlled |
| COOH | Carboxylic group |
| CT | Computed tomography |
| cm | Centimeter |
| $cm^2$ | Square centimeter |
| $cm^3$ | Cubic centimeter |
| CV | Coefficient of variation |
| dB | Decibel |
| DOL | Dosimetry laboratory |
| EPR | Electron paramagnetic resonance spectroscopy |
| FFF | Flattening filter free |
| $g$ | Spectrum center g-factor |
| G | Gauss |
| GHz | Giga Hertz |
| Gy | Gray |
| $h$ | Planck's constant |
| HU | Hounsfield unit |
| IAEA | International Atomic Energy Agency |
| ICRU | International commission on radiation units and measurements |
| IROC Houston | Imaging and radiation oncology core Huston |
| IMRT | Intensity-modulated radiation therapy |
| keV | Kilo electronvolt |
| MLCs | Multileaf collimators |
| min | Minute |
| MP | Microwave power |
| MA | Modulation amplitude |
| MU/min | Monitor unit per minute |
| MV | Megavoltage |
| OARs | Organs at risk |

| | |
|---|---|
| OSLD | Optically stimulated luminescence dosimeter |
| PSD | Plastic scintillation detector |
| PTV | Planning target volume |
| QA | Quality assurance |
| RPLGD | Radiophotoluminescent glass dosimeter |
| RTOG | Radiation therapy oncology group |
| SBRT | Stereotactic body radiation therapy |
| SD | Standard deviation |
| sec | Second |
| SRS | Stereotactic radiosurgery |
| SRT | Stereotactic radiation therapy |
| SSD | Source to surface distance |
| TC | Time constant |
| TLD | Thermoluminescent dosimeter |
| TPS | Treatment planning system |
| VMAT | Volumetric modulated arc therapy |
| W | Watt |
| $\nu$ | Microwave frequency |
| $|\mu_B|$ | Absolute value of the bohr magneton |

# CHAPTER 1

# INTRODUCTION

## 1.1 Background and Rationale

Radiation therapy is a type of cancer treatment that employs high radiation doses to destroy cancer cells and shrink tumors in a specific location. Cancer cells that are unable to repair themselves or reproduce new cells will die due to radiation, but normal cells that have been injured by radiation can recover themselves. Therefore, the medical physicist must always carefully plan the treatment for accurate dosage and targets to minimize the effect on normal cells or tissues. However, special radiation treatment techniques such as intensity-modulated radiation therapy (IMRT), volumetric modulated arc therapy (VMAT), stereotactic radiosurgery (SRS), stereotactic radiation therapy (SRT), as well as stereotactic body radiation therapy (SBRT) can treat cancer with advanced radiotherapy systems (Tomotherapy, Gamma Knife and CyberKnife).

As an alternative to surgery, stereotactic radiosurgery (SRS) uses image-guided radiation therapy for accurate dose delivery of single large doses to small tumors. This technique irradiates the target to achieve steep dose gradients outside the treatment volume while delivering a concentrated dose within the lesion. Every year, approximately 400,000 patients worldwide are diagnosed with intracranial metastases; about 70-80 percent of these patients will have multiple intracranial metastases (1). SRS treatment of multiple cranial metastases with a single isocenter has recently been increased, resulting in even shorter treatment periods. Because cone collimation can only treat one target at a time, multileaf collimators (MLCs) are frequently required. However, to minimize potential errors in treatment delivery that can lead to clinical complications, all radiotherapy processes should be subjected to appropriate quality assurance procedures, such as regular quality control testing and independent dosimetry audit.

The two largest audit networks are currently operated by the International Atomic Energy Agency (IAEA) (2, 3) and the Imaging and Radiation Oncology Core Huston (IROC Houston) (4, 5). Several works on SRS have studied anthropomorphic phantoms that are utilized for complex radiotherapy treatment quality assurance, audits, and trials (5-8). Moreover, the IAEA Dosimetry Laboratory (DOL) strives to enhance the accuracy of clinical dosimetry in worldwide hospitals by providing independent remote audits for high-energy photon beams. For the past forty-seven years, a thermoluminescent dosimeter (TLD), a passive dosimeter, has been commonly used and distributed to participating hospitals for auditing the accurate dose assessment by the IAEA DOL (2, 9), whereas optically stimulated luminescence dosimeter (OSLD) and radiophotoluminescent glass dosimeter (RPLGD) have emerged as new instruments to replace TLD for treatment accuracy audit among global hospitals (10-14).

End-to-end test is an approach for determining whether an application's flow is performing as designed from start to finish. It measures the overall geometric and dosimetric accuracy of the planning and treatment chain. The purpose of the end-to-end test is to ensure that the entire chain of radiation treatment, starting from imaging/simulation, treatment planning, monitor calibration, and beam delivery, is operable and leads to the desired results with sufficient accuracy. Usually, TLD, OSLD, and RPLGD dosimeters are used to assess the performance of the operation technique. The TLD has the advantage of being tissue equivalent and a transfer dosimeter that does not require electrical wiring for measurement. It is also available in various forms. On the other hand, TLD requires careful handling, complicated calibration, and fading correction. Moreover, the readout procedure has a large uncertainty. The OSLD has the benefits of high sensitivity, ease of operation, user-friendly, and repeated reading. However, the limitations of OSLD are energy dependence and not a tissue equivalent material. RPLGD offers good reproducibility

and linearity, repeated reading, and less fading than TLD, although it is not tissue equivalent.

Nevertheless, the alanine dosimeter is tissue equivalent and less fading. On the other hand, it is affected by ambient factors. Alanine is a neutral non-polar amino acid that exists in two structural forms: $\alpha$ ($CH_3$-CH($NH_2$)-COOH) and $\beta$ ($CH_2$($NH_2$) $CH_2$-COOH). It is one among the most common amino acids used in the human body for protein synthesis. Besides within the human body, alanine can also be used in radiation dosimetry (15). The $\alpha$-alanine is a universally used structure for radiation dosimetry because of the high stability of radiation-induced free radicals, while $\beta$-alanine is an improper structure for radiation dosimetry due to the low stability of radicals.

In addition, an alanine dosimeter is a transfer standard dosimeter (dosimeter with high metrological qualities suitable for conveying dose from an accredited/standard laboratory to an irradiation institution to establish traceability) used in high-dose dosimetry and to determine a wide range of radiation doses (16). Since alanine has a good response at high doses, it has been reported to benefit a stereotactic radiosurgery (SRS) of the intracranial treatment using radiation dose of 15-24 Gy (17). Furthermore, an alanine dosimeter has been used in high-dose dosimetry to calculate a wide range of radiation doses across various published studies on SRS (18-20). Other research studies on SRS have investigated anthropomorphic phantoms utilized for complex radiotherapy treatment quality assurance, audits, and trials (5-8). To the best of our knowledge, the alanine end-to-end test phantom has not been reported for SRS. Therefore, this study aims to develop an end-to-end test phantom for stereotactic radiosurgery (SRS) using an alanine dosimeter by fabrication of a head phantom and dosimetry insertion.

## 1.2  Research question

What is the dose accuracy of SRS VMAT plans in end-to-end test phantom using alanine dosimeter?

## 1.3  Research objective

To determine the dose accuracy of SRS VMAT plans in end-to-end test phantom using alanine dosimeter.

## 1.4  The scope of the thesis

This study covers the measurements of an end-to-end test phantom using an alanine dosimeter and optimization of EPR operation parameters in the radiotherapy range, including alanine characteristics, output survey, and fabrication of a head phantom for end-to-end test and validation.

จุฬาลงกรณ์มหาวิทยาลัย
CHULALONGKORN UNIVERSITY

CHAPTER 2

REVIEWS OF RELATED LITERATURE

## 2.1  Theories

### 2.1.1  End-to-end test

An end-to-end test is a methodology used to determine whether an application's flow is performing as designed from start to finish. End-to-end testing measures the overall geometric and dosimetric accuracy of the planning and treatment chain. The purpose of the end-to-end test is to ensure that the entire chain of radiation treatment, starting from imaging/simulation, treatment planning, monitor calibration, and beam delivery, is operable and leads to the desired results with sufficient accuracy.

### 2.1.2  Phantom

In this study, an end-to-end test phantom was designed to simplify geometries within a soft tissue equivalent material. The material used in phantoms should have the same density as the tissue. Dosimeter insertion contains an organ at risk (OAR) and the target which shall be inserted into the phantom for each dosimeter.

Here, a computer numerically controlled (CNC) was used to fabricate a head phantom. CNC is a computer-assisted procedure that uses instructions generated by a processor and stored in a memory system to control general-purpose machines. As shown in Figure 2.1, it is a subtractive manufacturing process that removes layers of material from a workpiece using computerized controls and machine tools to produce a custom-designed part. This process is utilized in various industries and applicable to various materials including metals, plastics, wood, glass, foam, and composites.
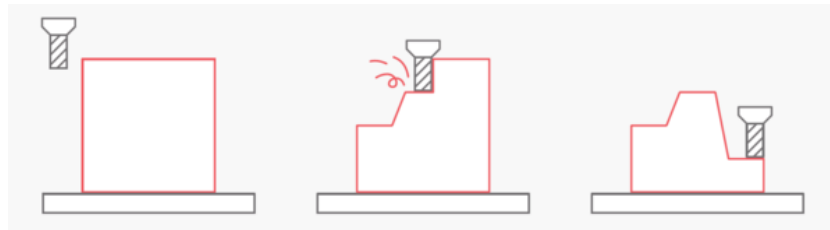
**Figure 2.1** subtractive manufacturing

### 2.1.3 Stereotactic radiosurgery or SRS

Stereotactic radiosurgery or SRS is a specialized technique in radiation therapy. SRS is an established non-invasive ablative treatment for brain metastases. It is an alternative to surgery that delivers accurate dose delivery of single large doses to small tumors. The image-guided radiation therapy is important to check the treatment's accuracy. This technique irradiates the target to achieve steep dose gradients outside the treatment volume while producing a concentrated dose within the lesion.

To limit movement and maintain the patient's comfort at all times during the treatment, a head frame or mask may be used. X-rays and measurements may be obtained before treatment to ensure that the patient is properly positioned. Depending on the type of SRS and the number of areas receiving SRS, setup and treatment time can range from 30 minutes to an hour.

Generally, for a single fraction to the 50 percent isodose line, prescription dosages for brain metastases range between 12 and 24 Gy. These doses are typically based on the findings of the Radiation Therapy Oncology Group (RTOG) 90-05 (17).

### 2.1.4 Volumetric modulated arc therapy

Volumetric modulated arc therapy (VMAT) is a special radiation treatment technique that continuously delivers radiation while the treatment machine rotates. Simultaneously, as illustrated in Figure 2.2, the multileaf collimator (MLC) moves dynamically and the dose rate and gantry speed vary continually. The treatment is

delivered using single or multiple arc rotations of the linear accelerator gantry. This technique precisely shapes the radiation dose to the tumor while minimizing the dose to the normal tissue surrounding the tumor. The VMAT technique is regularly used to treat tumors in head and neck, prostate, breast, pelvis, and other areas.
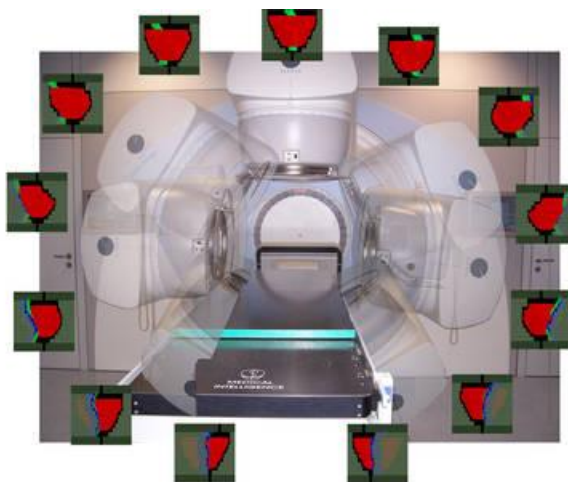


**Figure 2.2** VMAT technique

### 2.1.5 Alanine dosimeter

Alanine is a neutral non-polar amino acid that exists in two structural forms: $\alpha$ ($CH_3$-CH($NH_2$)-COOH) and $\beta$ ($CH_2$($NH_2$) $CH_2$-COOH). It is one of the most common amino acids used in the human body for protein synthesis. Besides the human body, alanine can also be used in radiation dosimetry (15). Due to high stability of radiation-induced free radicals, the $\alpha$-alanine is a universally used structure for radiation dosimetry, whilst $\beta$-alanine is an unsuitable structure for radiation dosimetry because of its low stability.
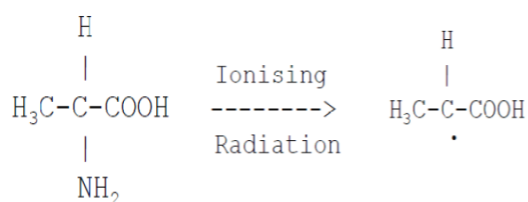


**Figure 2.3** The molecules interaction with radiation alanine

The interaction of the molecules with radiation alanine is depicted in Figure 2.3. The molecular structure of alanine is $CH_3CH(NH_2)$ COOH consisting of a carboxylic group (COOH), amino group ($NH_2$), and a methyl group ($CH_3$). All hydrogen atoms are bound to a central carbon atom. The weakest bond of alanine is C-N which is easily broken during the radiolysis, giving the $NH_3$ (ammonium, stable molecule) and SAR radical. Irradiation of alanine produces stable free radicals, the concentration of these radicals is proportional to the absorbed dose measured by Electron Paramagnetic Resonance (EPR) spectroscopy.

### 2.1.6  Electron Paramagnetic Resonance (EPR) spectroscopy
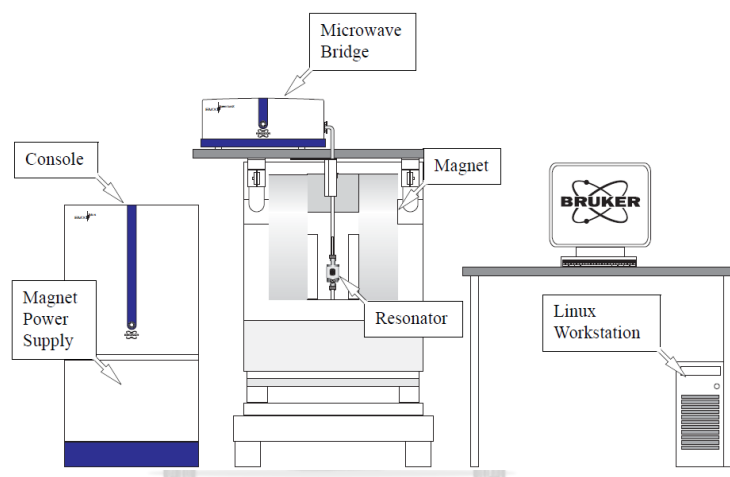


**Figure  2.4** The components of the EPR (21)

The components of the EPR are illustrated in Figure 2.4. EPR spectroscopy consists of three components: a source of electromagnetic radiation, a sample, and a detector. The microwave bridge box contains the electromagnetic radiation source and detector used to measure the EPR signal within the microwave bridge. A microwave resonator (or cavity) holds the sample and a metal box helps amplify weak signals from the sample. This section holds the sample while measuring the electron spin resonance signal. For the cavity's resonance frequency, no microwaves are reflected, but they remain inside the cavity. It also has a magnet for fine-tuning the electrical energy levels. Additionally, the console contains signal processing and

electronics control. A computer is used to analyze data and coordinate all the units involved in acquiring a spectrum. (21)
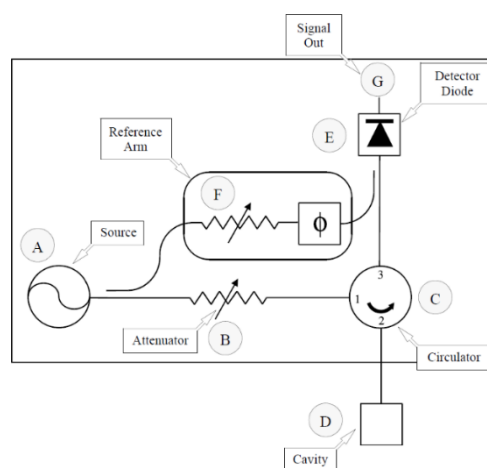


**Figure 2.5** Microwave bridge block diagram (21)

The block diagram of the microwave bridge is shown in Figure 2.5. The Microwave Bridge function (shown in A) generates microwave waves, and the detector (shown in B) measures the ESR signal within the microwave bridge. The cavity and sample (as shown in D) is the component that holds the sample to measure the electron spin resonance signal. The purpose of the cavity is to reflect the undisturbed microwave, allowing it to return to the microwave bridge.

The magnetic field is created by an electric current flowing through two conductor coils in the white circle area. The magnetic field's intensity can be adjusted by reducing the electric current flowing through the coil. At point A, the microwave is generated and divided into two paths. Path 1 is expected to reach the sample at point D, while path 2 is directed to the detector diode at point E for reference.

Path 1 transmits the microwave to point B, which is an attenuator that regulates the frequency of microwave power and the microwave. The microwave is directed to point C, and the device only transmits microwave waves from point B to point D. It also restricts microwave reflection to D and E. Microwave data for path 2 is collected and compared to the microwave that affects the sample at point F.

The detector diode (shown in E) converts the microwave power of both paths to an electric current, which is then compared to identify the difference so that the sample can absorb the microwave.

The result is depicted in the graph indicated in Figure 2.6. Nevertheless, interference from electronic devices, such as noise, must be considered because it can influence the results. This issue can be addressed by adjusting the magnetic field values with the same amplitude as the microwave power.
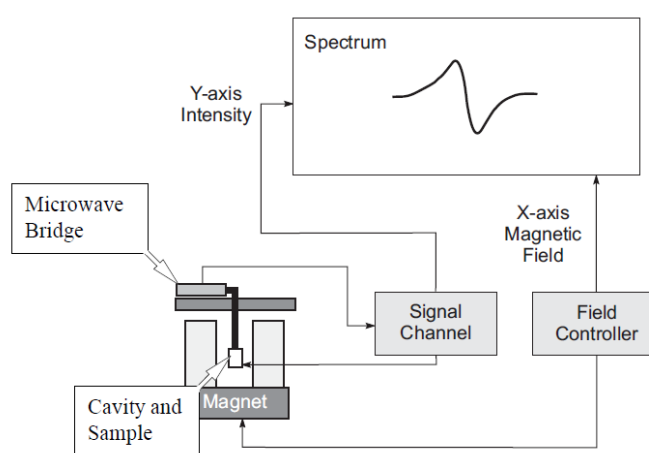


**Figure  2.6** An EPR spectrometer block diagram (21)

There are two techniques for measuring the spectral intensity (22); 1) the height difference between the maximum and minimum of a first derivative spectrum, which is the first approach commonly used, and 2) the area under the absorption curve is calculated using the double integral approach. Although the double integration approach is more fundamental, the height difference technique is simpler to use.

For EPR, the selection of the acquisition parameter for the spectrum can influence the quantitative determination of three parameters, namely, microwave power (MP), modulation amplitude (MA), and time constant (TC). As shown in Figure 2.7, both MP and MA affect the spectrum shape, resolution, and amplitude. Sensitivity initially increases with an increase in MP or MA and then decreases. The ESR amplitude at each point of the spectrum is averaged by expanding the time constant, reducing the influence of background noise caused by electronic devices.
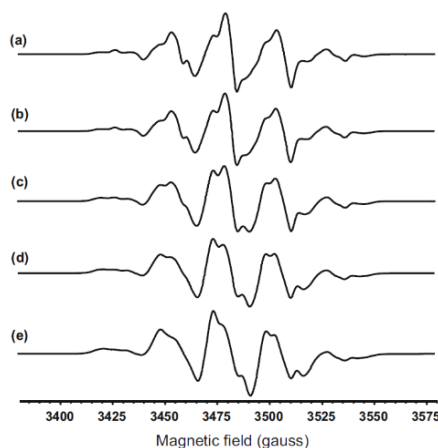
**Figure 2.7** EPR spectra of γ-irradiated alanine with microwave power values of (a) 0.15, (b) 1.5, (c) 10, (d) 22, and (e) 50 mW. All spectra were collected with modulation amplitude of 2 gausses, a conversion time, and a time constant of 20.48 ms (21).

### 2.1.6.1 Field sweep parameters and options (21)

The parameters for most experiments are divided into two panels as shown in Figure 2.8. The first panel is labeled with the name of the experiment, in this case field sweep. It contains the parameters that are most likely to be changed by the user. The second panel is labeled options and contains parameters that the user will seldomly change.
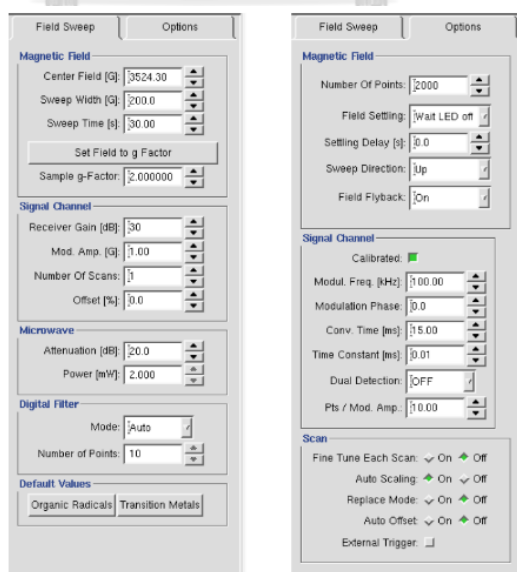


**Figure 2.8** Field sweep parameters and options (21)

### 2.1.6.1.1 Parameter for magnetic field

- Center field: the center field of the magnetic field sweep. The units are in gauss (G).

- Sweep width: the sweep width of the magnetic field sweep. The units are in gauss (G). The magnetic sweep range is center field - sweep width/2 to center field + sweep width/2.

- Sweep time: the time used to sweep from the beginning to the end of the magnetic field sweep. The units are in second (s).

- Set Field to g-factor: the g-factor and the microwave frequency determine the magnetic field at which the EPR signal appears and is given by:

$$\text{Field for resonance} = \frac{h\nu}{g|\mu_B|}$$

where h is Planck's constant, $\nu$ is the microwave frequency, g is the spectrum center g-factor, and $|\mu_B|$ is the absolute value of the Bohr magneton. If the microwave frequency is given in GHz and the magnetic field in Gauss, the center field is set to the field for resonance given by:

$$\text{Center field} = \frac{\nu \cdot 714.4775}{g}$$

### 2.1.6.1.2 Parameter for signal channel

- Receiver gain: the gain used in the signal channel. The units are in dB. The formula for the receiver gain is given by:

$$\text{Receiver gain} = log_{10}\left(\frac{V_{output}^2}{V_{input}^2}\right)$$

where $V_{output}$ is the output voltage and $V_{input}$, is the input voltage. The change in signal size has the following dependence on the receiver gain.

| Receiver gain change | Increase/Decrease in signal |
|:---:|:---:|
| +6 | 2 |
| −6 | 1/2 |
| +20 | 10 |
| −20 | 1/10 |

Note: this does not influence the data values because by default the values are normalized by the receiver gain.

● Mod. Amp.: the field modulation amplitude for acquiring the signal.

● Number of scans: this is the number of average when one is signal averaging.

### 2.1.6.1.3 Parameter for microwave

● Attenuation: this parameter is the microwave attenuation. The microwave source produces 200 mW and this power is then attenuated by the microwave attenuator. The microwave power is given by:

● Microwave Power (mW) = 200 ⋅ 10–Microwave Attenuation (dB)/10

● Power: the microwave power can be adjusted either by editing the Attenuation (described above) or directly entering a microwave power.

### 2.1.6.1.4 Parameter for digital filter

● Mode: there are two modes for digital filtering, auto and manual modes. It is set to auto by default.

● Number of points: the number of points used in digital filtering.

## 2.2 Review of related literature

Several research works on SRS have studied Anthropomorphic phantoms utilized for complex radiotherapy treatment quality assurance, audits, and trials. The majority of the researchers assembled novel parts for multiple instruments in commercial anthropomorphic phantoms.

Dimitriadis A et al. (23) used three detectors in their study in 2017: Exradin W1 plastic scintillation detector (PSD), Gafchromic$^{TM}$ EBT-XD, and alanine dosimeter. Accordingly, a STE$_2$EV phantom (CIRS, Norfolk, VI) was used where two insertions were created for dosimetry and target. The target insertion was a resin-based 3D printed cube consisting of PTV and OAR. The PTV was designed for brain metastasis about 8 cm$^3$ in size, while the OAR was similar to the brainstem and thalamus in size and shape. The dosimetry insertion consisted of three pieces of brain equivalent material and had the same dimensions as the target insertion. Due to the detector's small and water-equivalent sensitive volume, which was difficult to visualize on CT scans, the quantification of the PSD position was not achievable in this investigation. For PTV, the results suggested that the dose difference between measured and TPS for PSD and alanine was 0.4% and in OAR was 19.8% for PSD, and 18.6% for alanine pellet 1, respectively. Furthermore, the agreement between the PSD and alanine pellet 1 was 0.4%, while the agreement of alanine pellet 1 in the OAR was within 1.2%. This article presented a three-detector combination for simultaneous measurement in a commercial anthropomorphic phantom, resulting in a phantom-detector system and a technique suitable for an end-to-end SRS dosimetry audit.

In addition, in 2019, Loughery E et al. (24) presented the findings of three institutional evaluations of an end-to-end test for conventional linacs treatment chains utilizing Integrated Medical Technologies' head-and-neck phantom (Troy, NY). Here, the RTOG 0022 protocol was employed along with 2-arc VMAT or 8-field coplanar IMRT, while OSLD (microStar2) and ion chamber (A1SL) detectors as well as solid epoxy head phantom were used. They found that the standard deviations reflect this lack of familiarity in institutions, with OSLDs having a greater overall

standard deviation (2.47%) than ion chambers (1.66%). They discovered the agreement among three institutions that passed the IROC Houston head-to-head to be credentialing.

Moreover, in 2019, Wesolowska P et al. (25) tested the approach for an end-to-end dosimetric audit of IMRT/VMAT. This investigation was conducted at IAEA multicenters on a countrywide scale. This work created a specified phantom out of polystyrene, while the IMRT QA was constructed from solid water HE. TLD-100 and Gafchromic EBT3 film detectors were used. According to the findings of the multicenter study, acceptance limits of 5% for dose measurements in PTV and 2.8 Gy dose threshold for dose measurements in OAR were proved to be feasible. The multicenter pilot study and national proceeds demonstrated that the IMRT/VMAT dosimetric end-to-end audit approach can be implemented with minimal challenges.

Meanwhile, the two major audit networks are the International Atomic Energy Agency (IAEA) (2, 3) and the Imaging and Radiation Oncology Core Huston (IROC Houston)(4). They have been conducting extensive studies on the traditional dosimeters in end-to-end testing such as TLD, OSL, and RP glass dosimeter, as well as the standard imaging Lucy 3D, CIRS STEEV phantom (1) and RUBY phantom (5-8). Several SRS investigations have also been undertaken along with the assessment of anthropomorphic phantoms used for complex radiotherapy treatment quality assurance, audits, and trials.(9-12) Moreover, an alanine dosimeter has been utilized in high-dose dosimetry to determine a wide range of radiation doses in numerous published studies on SRS.(14-17) Due to a good response at high doses, alanine is beneficial to be used in stereotactic radiosurgery (SRS), which is an intracranial treatment employing radiation dose of 15-24 Gy (7). To the best of our knowledge, there is no study on the use of alanine dosimeters for end-to-end measurement in Thailand till date.

SRS necessitates precise and accurate dose delivery verification procedures. Consequently, a quality assurance program for SRS must be established at Thailand's

new cancer center. Moreover, the intricacy of VMAT as well as highly qualified and multidisciplinary clinical staff must be considered. Therefore, an end-to-end test is required.

In addition, no end-to-end test for SRS has been established in Thailand. While alanine dosimeter has limited application in radiotherapy, this study will focus on the use of alanine in SRS for a single fraction large dose.

# CHAPTER 3

## RESEARCH METHODOLOGY

### 3.1 Research question

What is the dose accuracy of SRS VMAT plans in end-to-end test phantom using alanine dosimeter?

### 3.2 Research objective

To determine the dose accuracy of SRS VMAT plans in end-to-end test phantom using alanine dosimeter.

### 3.3 Research design

This study is an observational descriptive study.

### 3.4 Conceptual framework

The factors that affect the dose accuracy are treatment machine, energy, treatment planning system, dose calculation algorithm, dosimeter, technique, and phantom. Figure 3.1 depicts the conceptual framework diagram.
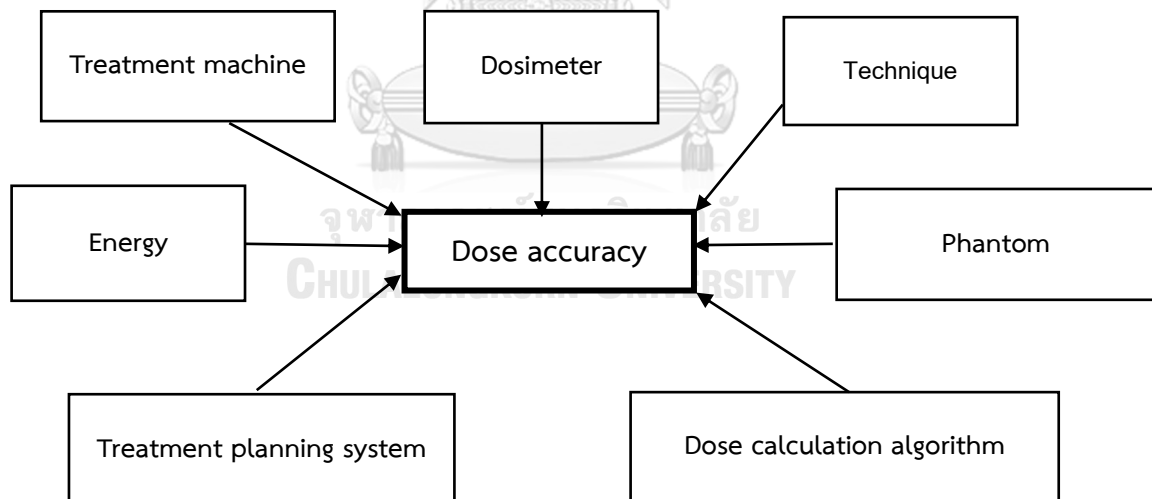


**Figure  3.1** Conceptual frameworks

## 3.5  Research design model

This research design has been divided into four main sections, which are EPR optimization, alanine characteristics, output survey, and end-to-end phantom fabrication and validation. Figure 3.2 illustrates the research design model in this study.
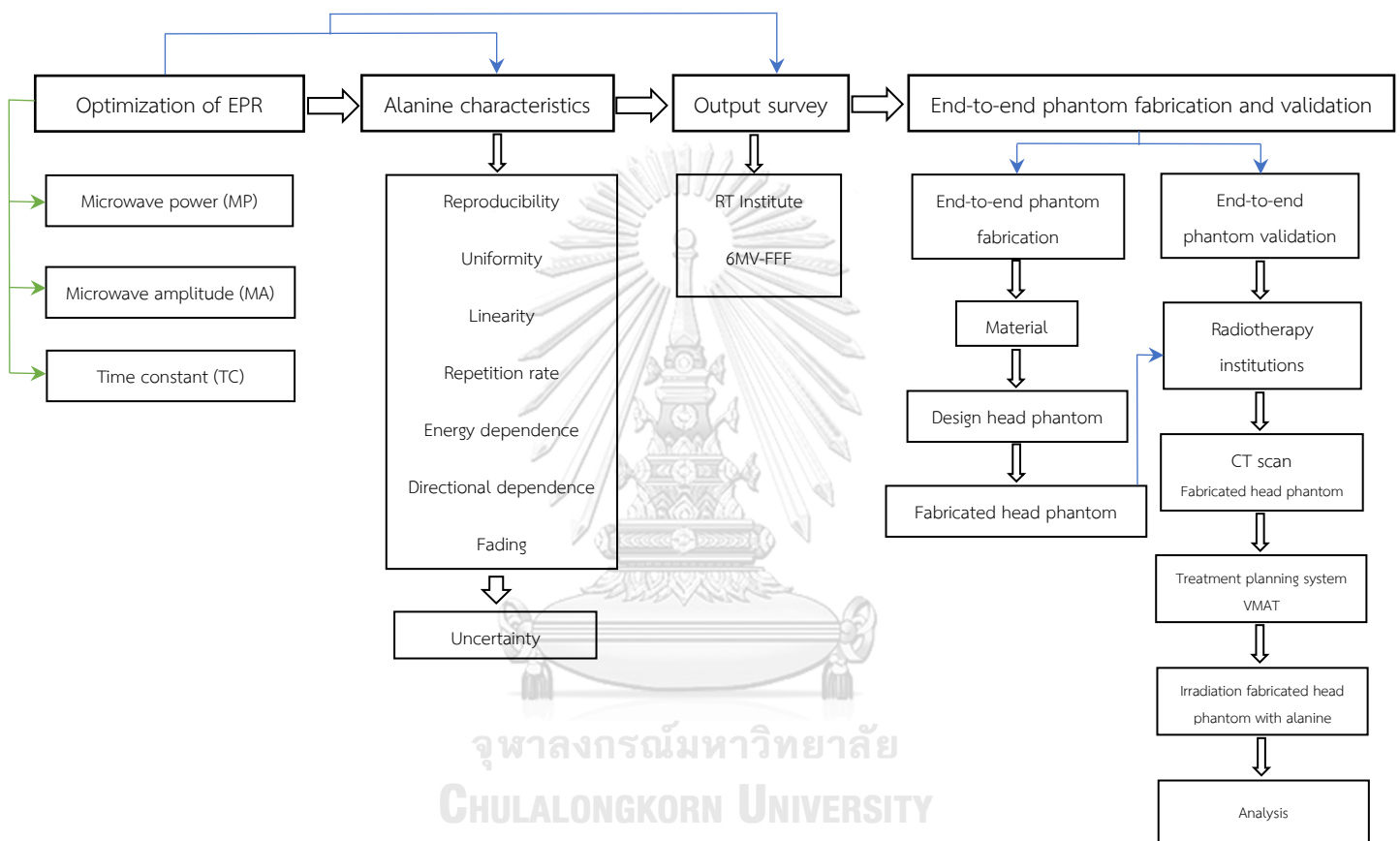


**Figure  3.2** Research design model

## 3.6  Keyword

- ➢ End-to-end test
- ➢ Head phantom
- ➢ SRS
- ➢ Alanine dosimeter
- ➢ VMAT

## 3.7 The sample

### 3.7.1 Target population

This study was conducted in a radiotherapy center that uses a linear accelerator from the Varian Medical System.

### 3.7.2 Sample size determination

The sample size was determined using the formula as equation (3.1).

$$n = \frac{z_{\alpha/2}^2 \times \sigma^2}{E^2}$$

.......................... (3.1)

where, n = number of repetitions

$$Z_{\alpha/2} = 1.96$$

Figure 3.3 shows that at 95% the confidence level, $\alpha$ = 1 – 0.95 = 0.05, hence z-critical value = 1.96.
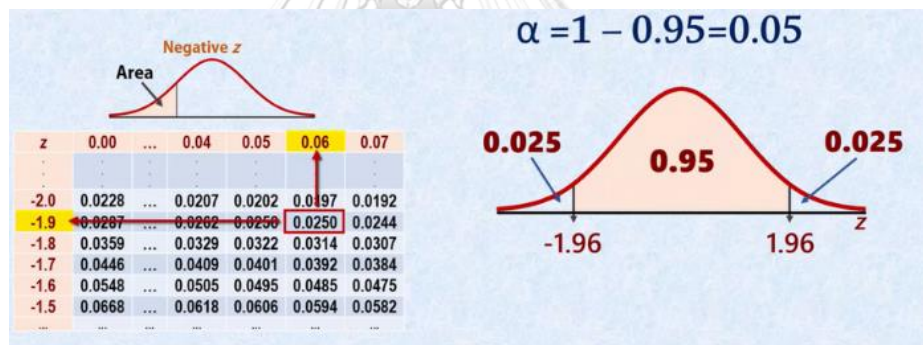


**Figure 3.3** The value of $Z_{\alpha/2}$ at 95% the confidence level

$\sigma$ = standard deviation of the alanine dosimeter uncertainty= 0.165 (From preliminary results of alanine uncertainty budget)

E = the margin of error = 0.36 (From 2% of prescribed dose 1800 cGy)

$$n = \frac{(1.96^2 \times 0.165^2)}{0.360^2} = 0.807$$

Therefore, n = 0.807 and a minimum of one repetition at a radiotherapy center is required in this study, while the measurement was performed at least twice.

## 3.8  Material

### 3.8.1  Linear accelerator

The Varian TrueBeam$^{TM}$ linear accelerator (Varian Medical System, Palo Alto, CA, USA) was employed in this study, as illustrated in Figure 3.4. The machine can be operated in 6MV, 10MV, 6MV-FFF, and 10MV-FFF for photon beams, and 6, 9, 12, 15, 18, and 22 MeV for electron beams. The range of field sizes is from 0.5x0.5 cm$^2$ to 40x40 cm$^2$ at the isocenter. The repetition rates ranged from 100 to 600 MU/min for conventional mode with flattening filter and maximum dose rate of 1400 MU/min for 6MV-FFF, and 2400 MU/min for 10MV-FFF. Here, the 6MV-FFF energies and dose rate of 1400 MU/min were used.



**Figure  3.4** The Varian TrueBeam$^{TM}$ linear accelerator

### 3.8.2  Solid water phantom

Solid water phantom (GAMMEX RMI, WI, USA) with a density and average atomic number of 1.03 g/cm$^3$ and 5.96, respectively, was used. The dimension was 30×30 cm$^2$, with thicknesses ranging from 0.2 to 5.0 cm, as shown in Figure 3.5.

**Figure 3.5** Solid water phantom

### 3.8.3 Alanine dosimeter

The alanine dosimeter consisted of 90.9% L-alpha-alanine and 9.1% paraffin wax as a binder. These dosimeters are 4.8±0.1 mm in diameter and 2.8±0.1 mm in height, with a total mass of 60±2 mg in the batch, and ±0.6 mg in the lot (standard deviation of 0.3 mg). This study used alanine batch number BY616 from Harwell Dosimeter Ltd., as shown in Figure 3.6.



**Figure 3.6** Alanine dosimeter

### 3.8.4 Electron Paramagnetic Resonance spectroscopy (EPR)

The EPR spectroscopy (Bruker BioSpin Corporation, Billerica, MA, USA) model EMXmicro was used, as indicated in Figure 3.7. This system is composed of a microwave bridge, resonator or cavity, console, magnet, magnet power supply, and Linux workstation. The microwave bridge is used to measure the EPR signal within the microwave bridge. The sample is in a resonator (cavity), which helps to amplify weak signals from the sample. Signal processing and electronics control are housed in the console. A computer is used for data analysis as well as coordinating all the units in acquiring a spectrum.
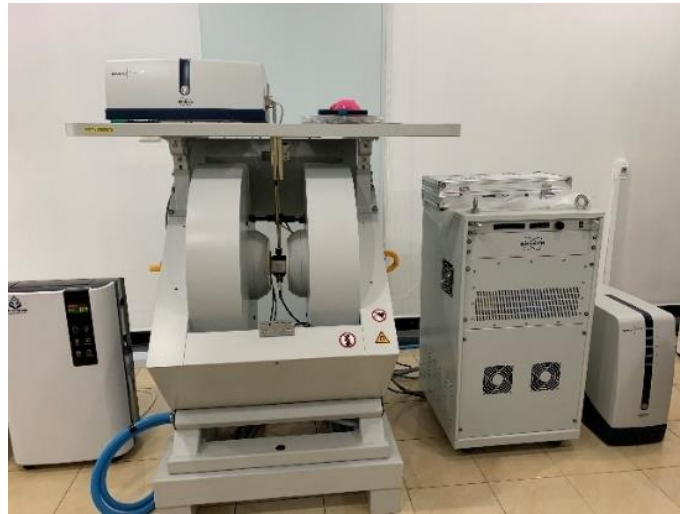
**Figure  3.7** Electron paramagnetic resonance spectroscopy (EPR).

### 3.8.5  Fabricated head phantom

Cast nylon was used in the fabrication of head phantom because it has a CT number of approximately 56 - 95 HU (26), which is close to that of soft tissue. The head phantom has dimensions of 15 cm diameter and 17 cm height, which were drilled for the dosimetry box consisting of 5 slice pieces: 4 slices for alanine of 1 cm height each and 1 slice for film of 2 cm height, as illustrated in Figure 3.8.
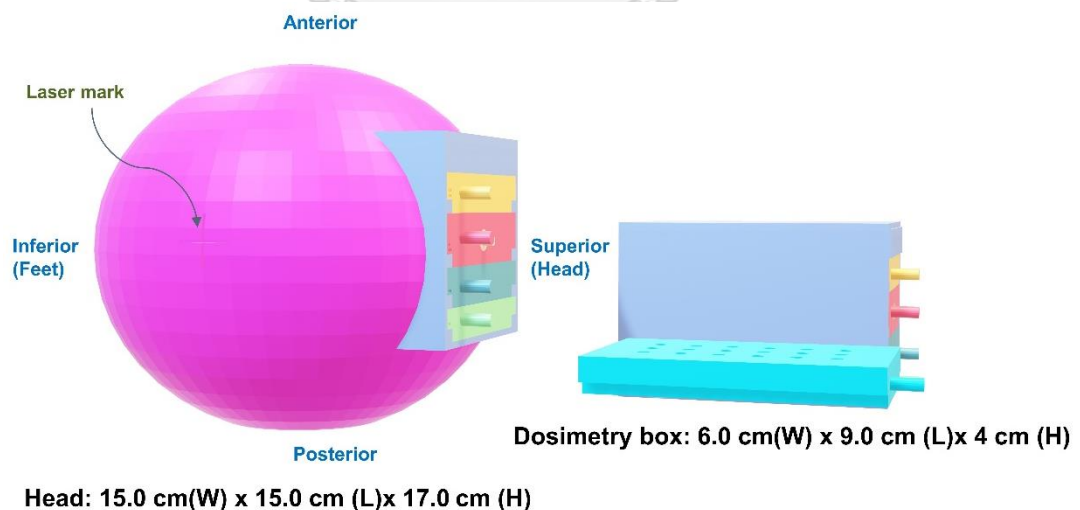


**Figure  3.8** Fabricated head phantom

**3.9 Method**

The irradiation of alanine dosimeters was performed with a 6MV-FFF beam generated by a linear accelerator, TrueBeam (Varian Medical System, Palo Alto, CA, USA). The study was divided into four sections, where the first section was the optimization of EPR operation parameters at radiotherapy level in the range of 100 – 2000 cGy, followed by alanine characterization in the second section. The third section was the output survey which was performed at eight radiotherapy centers in Thailand. Finally, the last section was end-to-end phantom fabrication and validation.

**3.9.1 Section I: Optimization of EPR operation parameter**

This section was performed to explore suitable EPR operation parameters. For EPR, the selection of the acquisition parameter for the spectrum can influence the quantitative determination, the three parameters include microwave power (MP), modulation amplitude (MA), and time constant (TC). Both MP and MA affect the spectrum shape, resolution, and amplitude, while TC influences the background noise due to electronic devices. For dose estimation, the difference between the maximum and the minimum of the ESR spectrum was performed using the height method (peak-to-peak amplitude) (27). To achieve a clear signal, MP was firstly investigated, followed by MA and time constant TC, respectively. The first parameter was MP, followed by MA using the MP value from the first step. The last parameter was TC using the MP and MA values from the earlier steps. Moreover, the other acquisition parameters were set as follows:

- center field: 3500 G
- sweep width: 200 G
- modulation frequency: 100 kHz
- sweep time: 40.45 s
- receiver gain: 30 dB
- number of scans: 3 times

Initially, in order to find MP, MA was fixed at 7.018 G as described in the previous study (27). To achieve a clear signal, MP will firstly investigated, followed by

MA and time constant TC, respectively. The first parameter will MP, followed by MA using the MP value from the first step. The last parameter will TC using the MP and MA values from the earlier steps. Moreover, the other acquisition parameters will be set as follows:

- center field: 3500 G

- sweep width: 200 G

- modulation frequency: 100 kHz

- sweep time: 40.45 s

- receiver gain: 30 dB

- number of scans: 3 times

Initially, in order to find MP, MA will be fixed at 7.018 G as described in the previous study (28) and TC was fixed at the minimum of 0.01 msec. Subsequently, MP was varied from minimum to maximum (5 to 35 dB, by increasing 1 dB in each step) and acquisition parameters described above were utilized at doses of 100, 300, 500, 1000, and 2000 cGy. As illustrated in Figure 3.9 (red line), the spectrum from the EPR signal was being observed until a clear spectrum was seen. The optimal MP was being recorded for each dose at this point. Finally, the MP square of all doses against the EPR intensity graph was plotted.
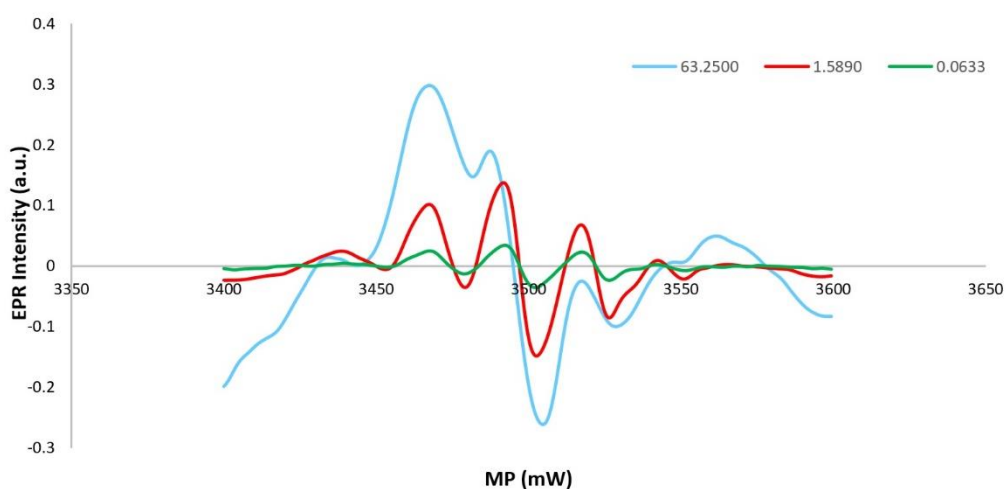
**Figure 3.9** Spectrum from EPR signal at dose delivery of 1 Gy was set at 5 dB (0.0633 mW), 21dB (1.589 mW), and 35 dB (63.250 mW). MA and TC were fixed at 7.018 G and 0.01 ms, respectively. Clear spectrum of alanine was present in the red line.

Following the preceding, MA was used as the acquisition parameter. The optimal MP found in the first measurement was used as a fixed parameter, while TC was fixed at the minimum of 0.01 msec. MA values were set at 1.000, 2.000, 2.999, 4.000, 5.000, 6.006, 6.579, 7.018, 7.576, 8.032, 8.584, 9.050, 9.569, and 10.050 G (this is a fixed MA step of EPR machine which user cannot adjust). Figure 3.10 (red line) shows the spectrum from EPR signal until a clear spectrum was observed. The optimal MA was being recorded for each dose at this point. Finally, the MA in units of G were plotted against the EPR intensity for all doses, whereas MA was used in one step from 1 to 10 G at dose 100, 300, 500, 1000, and 2000 cGy.
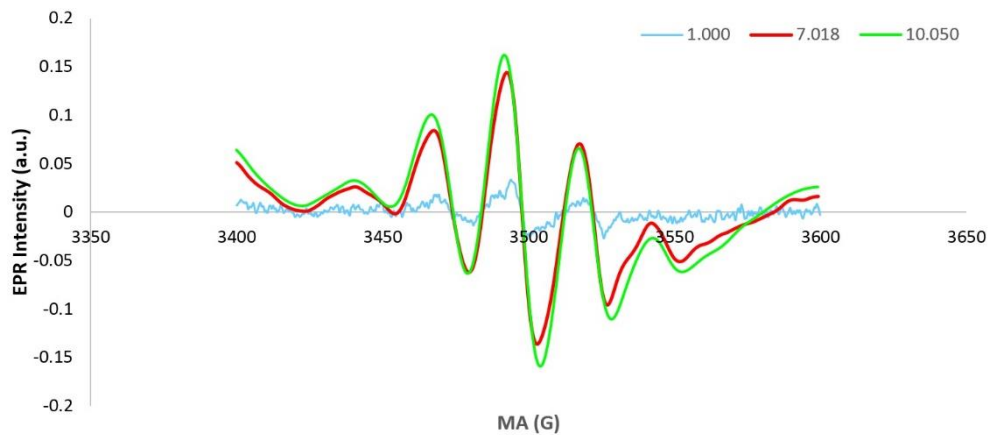
**Figure 3.10** Spectrum from EPR signal at dose delivery of 100 cGy was set at 1.000, 7.018, and 10.050 G. Optimal MP was 1.589 mW and TC was fixed at 0.01 ms. Clear spectrum of alanine was present in the red line.

Lastly, the optimal MP and MA obtained from above procedures were used as fixed parameters to set TC at 0.01, 0.02, 0.04, 0.08, 0.16, 0.32, 0.64, 1.28, 2.56, 5.12, 10.24, 20.48, 40.96, 81.92, 163.84, 327.68, 655.36, 1310.72, 2521.44, and 5242.88 msec (this is a fixed TC step of EPR machine which user cannot adjust). As indicated in Figure 3.11, the EPR signal was observed, and the peak-to-peak width ($\Delta$BPP) was measured. Each $\Delta$BPP was normalized to $\Delta$BPP of TC 0.01 msec at doses of 100, 300, 500, 1000, and 2000 cGy.
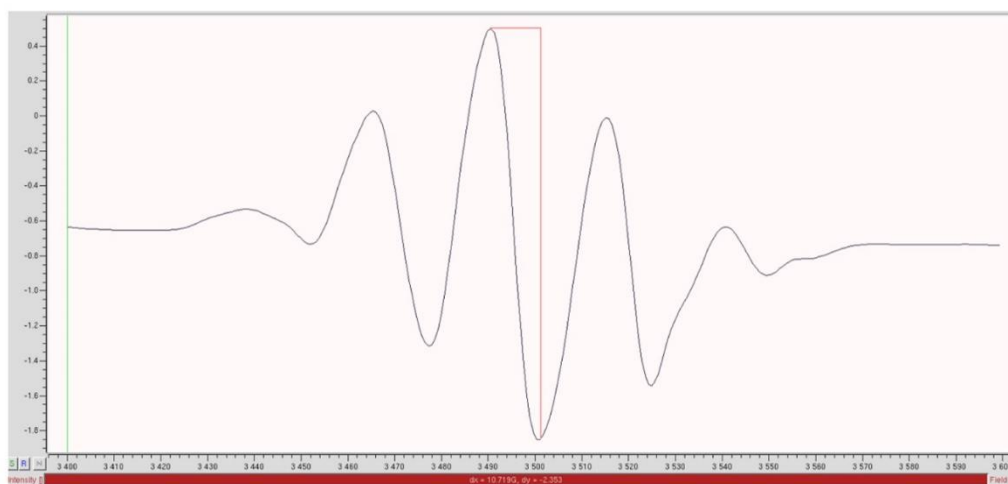


**Figure 3.11** Measured EPR signal shown in red line for peak-to-peak width ($\Delta$BPP) at TC=40.96 Ms of dose 1000 cGy

### 3.9.2  Section II: Alanine characteristics

After EPR operation parameter optimization from the first section, this section was performed to examine the characteristics of alanine. The measurements were conducted to examine seven characteristics, namely uniformity, reproducibility, linearity, repetition rate, energy dependence, directional dependence, and fading. The data was employed to estimate the uncertainty of alanine.

#### 3.9.2.1  The irradiation setup

This measurement was performed at 6MV-FFF (Flattening filter free) beam generated by a linear accelerator, 100 cm source to surface distance (SSD), and a field size of 10x10 cm$^2$ at 100 to 2000 cGy. The 6 MV was chosen because it provides a better beam profile with less transmission penumbra than 10MV, and FFF is a standard approach for reducing irradiation time during patient treatment. A beam size of 10x10 cm$^2$ can ensure that all dosimeters are irradiated. Here, a set of each dose is represented by five alanine dosimeters in a plastic bag. Figure 3.12 shows a package inserted between 1 cm bolus thickness to reduce the air gap effect in the solid water phantom.
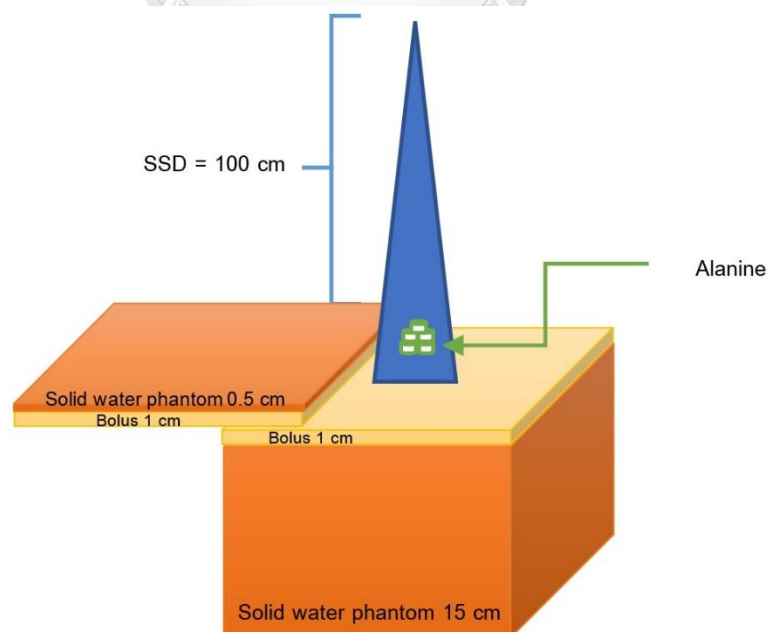


**Figure  3.12** The alanine dosimeter setup irradiation

### 3.9.2.2  Uniformity

Ten alanine pellets were irradiated at the same time with 1000 cGy at 6 MV-FFF, 100 cm SSD, with a field size of 10 x 10 cm$^2$ at 1.5 cm depth. EPR intensity was read at each alanine pellet. The batch uniformity of all alanine dosimeters was determined by the average EPR intensity of 10 alanine pellets.

### 3.9.2.3  Reproducibility

The ten alanine pellets from uniformity measurement were used. The reproducibility was determined by the average EPR intensity of five times readout for each alanine pellet.

### 3.9.2.4  The linearity

The ten alanine pellets were irradiated in five doses of 100, 200, 500, 1000, 2000, and 3000 cGy from 6MV-FFF, 100 cm SSD, with a field size of 10 x 10 cm$^2$ at 1.5 cm depth. The calibration curve was established. The readout of alanine pellets was averaged from EPR intensity of ten alanine pellets (a.u.) as dose (Gy).

### 3.9.2.5  Repetition rate

To study the response of alanine against high MU rate, five alanine pellets were irradiated with 1000 cGy from 6MV-FFF, 100 cm SSD, with a field size of 10 x 10 cm$^2$ at 1.5 cm depth. The responses were performed at 400, 800, 1200, and 1400 MU/min, respectively. The readout of alanine pellets was averaged from EPR intensity of five alanine pellets at each repetition rate. Finally, the repetition rate in each measurement was normalized to 1400 MU/min.

### 3.9.2.6  Energy dependence

Five alanine pellets were irradiated with 1000 cGy, 100 cm SSD, with a field size of 10 x 10 cm$^2$ at 1.5 cm depth from 6MV, 6MV-FFF, as well as at 2.5 cm depth from 10MV, and 10MV-FFF. The repetition rate for 6MV was performed at 600 MU/min, while the repetition rate for 6MV-FFF, 10MV, and

10MV-FFF was achieved at 1400 MU/min. The readout of alanine pellets was the average EPR intensity of five alanine pellets in each measurement and was normalized to 6MV-FFF.

### 3.9.2.7 Directional dependence

The five alanine pellets were irradiated with 1000 cGy, 100 cm SSD, with a field size of 10 x 10 cm$^2$ at 1.5 cm depth from 6MV-FFF for directional dependence. The alanine dosimeter was placed between 1 cm thickness of bolus. This was performed in two directions, perpendicular and parallel, as illustrated in Figure 3.13, where parallel measurements were normalized to perpendicular direction.



Photon beam                Photon beam

Alanine                    Alanine

**Perpendicular**              **Parallel**
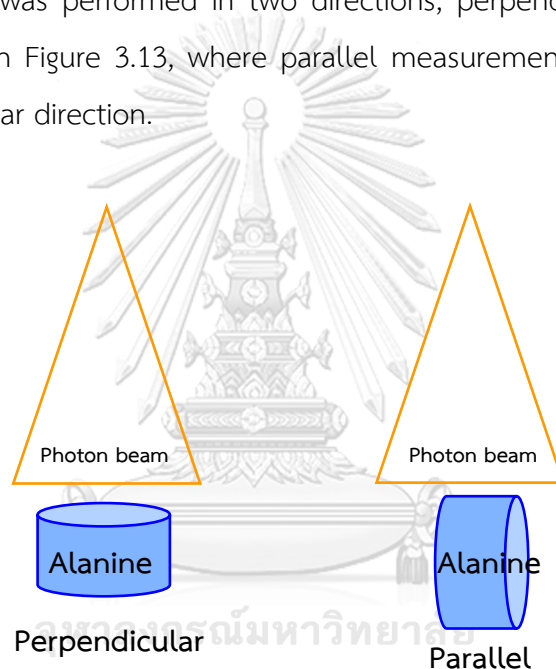
**Figure 3.13** The direction of alanine

### 3.9.2.8 The fading

For fading determination, sixty alanine pellets were exposed to 1000 cGy from 6MV-FFF 100 SSD cm, with a field size of 10 x 10 cm$^2$ at 1.5 cm depth. Five alanine pellets were separated for readout measurement for 12 consecutive weeks.

The other alanine pellets were stored in a dry cabinet at room temperature. The fading determination was defined as the response of EPR intensity to the initial EPR intensity readout.

### 3.9.2.9  The uncertainty

The uncertainty of alanine was calculated following the "Guide to the expression of uncertainty in measurement" (JCGM100:2008) (29).

### 3.9.3  Section III: Output survey

This section was performed to investigate the validation of alanine dosimeter after measurement was completed in sections I and II. Each radiotherapy center has a 6MV-FFF linear accelerator for this measurement. An output survey was performed in eight radiotherapy centers by proceeding as follows:

- Three sets of alanine were sent by mail service to each radiotherapy center.

- Each set contains five alanine pellets. Since each radiotherapy center received three sets of alanine, uncertainty was measured by irradiating with two sets of alanine dosimeters, while the other set was used for background, which records environmental influences during transport and storage.

- The output measurement was performed in solid water phantom. The delivery dose was at 1000 cGy of 6 MV-FFF. The field size is 10 x 10 cm$^2$ at a depth of $D_{max}$. The alanine dosimeter was placed between 1 cm thickness of bolus to reduce the air gap effect in the solid water phantom.

- Within two weeks of the irradiation, the alanine was returned to the King Chulalongkorn Memorial Hospital through mail service, and these dosimeters were evaluated.

### 3.9.4  Section IV: End-to-end phantom fabrication and validation

This section was performed to fabricate the head phantom and validate it by using an alanine dosimeter for an end-to-end test in SRS. The measurement was divided into two parts: fabrication of the head phantom and validation of the fabricated head phantom.

### 3.9.4.1 Fabrication of head phantom

#### 3.9.4.1.1 Material for fabrication

This process identified the material for fabrication, design, and fabrication of the head phantom.

The phantom material was created using a preliminary set of various materials as shown in Table 3.1.

**Table 3.1** Preliminary phantom materials for this study.

| Material | Density (g/cm³) | CT Number (HU) (This study) | CT Number (HU) (Other studies) |
|---|---|---|---|
| PLA | 1.14 | 213 | 13.0 ± 144.3 (30) |
| | | | 125 (31) |
| Epoxy Resin (3D-printed) | 1.11 | 73 | 69.2 (32) |
| Cast Epoxy Resin | - | 91.6 | - |
| Cast Resin | - | 155.2 | - |
| ABS | 1.04 | - | -30 – 25 (33) |
| HDPE | 0.97 | - 85.2 | - |
| PMMA | 1.17 | - | 92 – 118 (26) |
| **Cast Nylon** | **1.14** | **80-100** | **56 – 95 (26)** |
| Nylon | 1.14 | 123.5 | - |

This study was specifically designed for an end-to-end test to measure alanine dosimeter using cast nylon because it has a CT number of about 56

- 95 HU (26), which is close to that of the soft tissue. Since nylon has a density of 1.14 g/cm$^3$, it is robust and portable to different radiotherapy centers.

### 3.9.4.1.2  Designing the head phantom

• The head phantom has a dimension of 15 cm diameter and 17 cm height, drilled for a dosimetry box consisting of five alanine slice pieces: four alanine slice pieces each of 1 cm height, and one slice for film of 2 cm height, as illustrated in Figure 3.14 and 3.15. The head phantom of 15 cm in diameter was selected to represent the diameter of an adult patient's head.
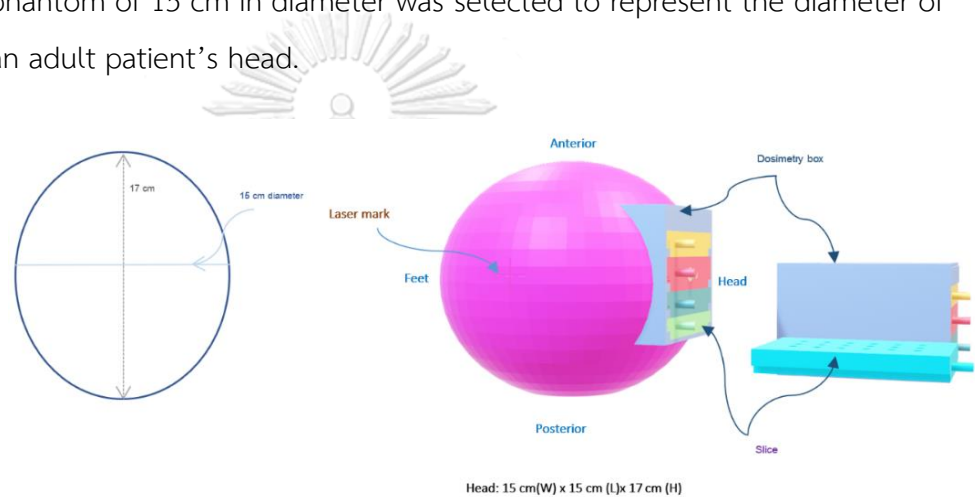


**Figure 3.14** Fabricated head phantom
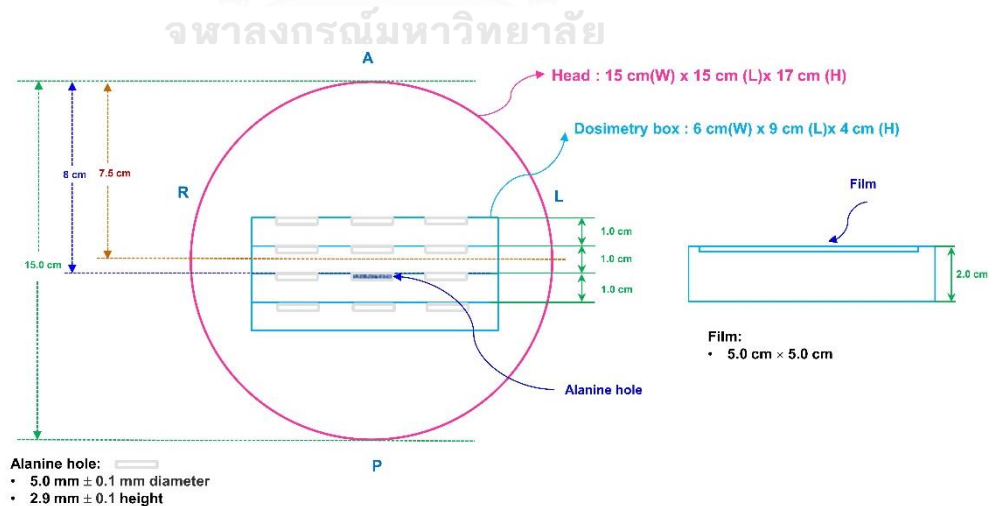


**Figure 3.15** Cross-sectional view of the phantom

● The film slice was drilled with an edge dimension of 5x5 cm$^2$ for a film to position axially within the target and the organ at risk (OAR) on the top of this slice as illustrated in Figure 3.15.

● The alanine slice contains 15 holes, each being 1 cm apart from the border and from one another. Pieces of cast nylon were placed to fill the gap in each hole. The alanine pellets were inserted in alanine slices and positioned at two measurement points, one in the target volume and one in the OAR representing the brain stem, with one alanine pellet used at each measurement position. As illustrated in Figure 3.16, the dimensions of OAR and the target are the same: 5.0± 0.1 cm diameter and 2.9±0.1 cm height.
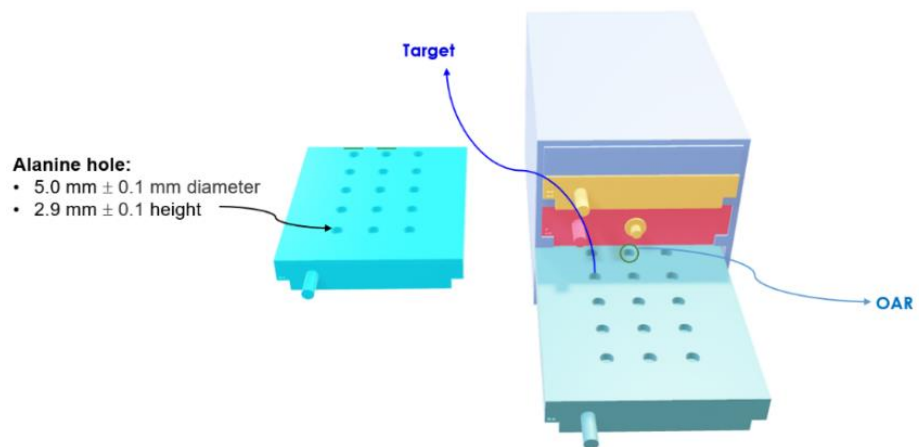


**Figure 3.16** Dosimetry slice for alanine

● A head phantom containing an OAR and the target is inserted into the phantom to allow placement of an alanine dosimeter. The OAR and target are of 5±0.1 cm diameter and 2.9±0.1 cm height.

● Laser alignment marks allow positioning at the isocenter based on room lasers.

### 3.9.4.1.3 Fabricated head phantom

In this study, the head phantom was created by computer numerically controlled (CNC) because CNC is appropriate for homogeneous materials, including a wide range of materials and sizes. This phantom was created by a CNC three-axis vertical machining center. Figure 3.17 shows the design of the fabricated cast nylon end-to-end test head phantom, CNC fabrication parts of the cast nylon, and the completed head phantom.
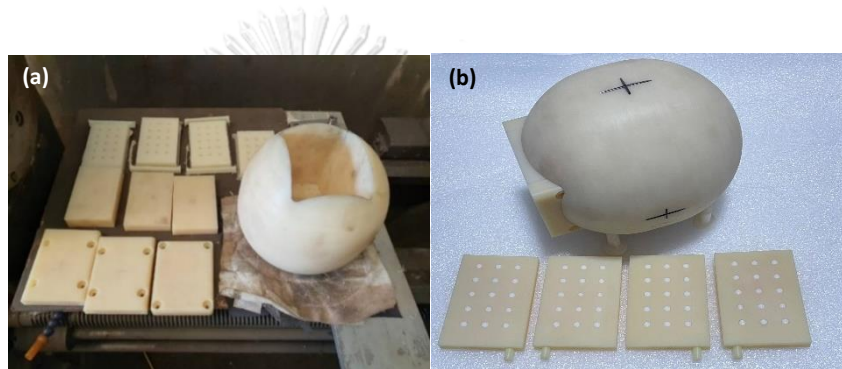


**Figure 3.17** (a) fabricated cast nylon head phantom parts using CNC technique, consisting of head drilled sphere for head phantom and alanine box set, and (b) completed set of fabricated cast nylon head phantom.

### 3.9.4.2 Validation of the fabricated head phantom

### 3.9.4.2.1 Material for the fabricated head phantom

This process was performed by scanning a set of the fabricated phantom in a CT simulator (GE HealthCare Chicago, IL, USA) with a slice thickness of 1.25 mm at 120 kVp as shown in Figure 3.18.
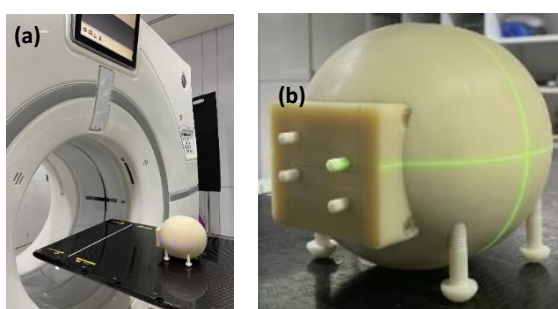
**Figure  3.18** Characterization of fabricated cast nylon head phantom using CT simulator (a) phantom setting and (b) phantom alignment.

### 3.9.4.2.2  End-to-end phantom validation

As shown in Figure 3.19, this process was performed to validate the fabricated head phantom. According to RTOG 90-05 (17), the prescribed dose to target was 1800 cGy based on acute and chronic toxicities but was 2100 cGy based on acute toxicity alone. The maximum tolerated dose (MTD) for the lesion was 21 - 30 mm in size. In this part was performed 3 measurements of the fabricated head phantom        end-to-end test which starting from CT imaging, treatment planning for contoured target and OAR, all plans were optimized with a dose of 1800 cGy, the AAA was used to calculate the dose, alanine pellets were placed in this phantom and irradiated according to the plan.
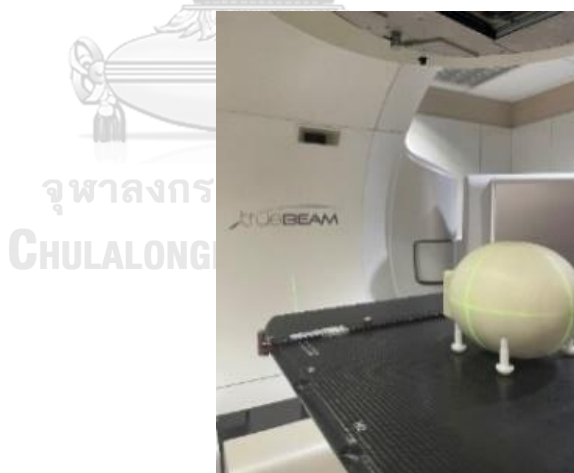


**Figure  3.19** Irradiation of fabricated head phantom with a set of alanine dosimeters inside the TrueBeam with 6 MV-FFF linear accelerator.

- Starting with CT scanning of the fabricated head phantom, the fabricated head phantom was scanned using a GE CT simulator (GE HealthCare Chicago, IL, USA) with a slice thickness of 1.25 mm at 120 kVp as shown in Figure 3.18.

- Next, the CT images were imported in the Eclipse (Varian Medical System Inc, Palo Alto, CA, USA) TPS for contouring of target and OAR of 7.9 $cm^2$ (x=2 cm, y= 2.5 cm) as shown in Figure 3.20
  - Positions 1 and 2 represent the target.
  - Positions 3 and 4 represent the brain stem.
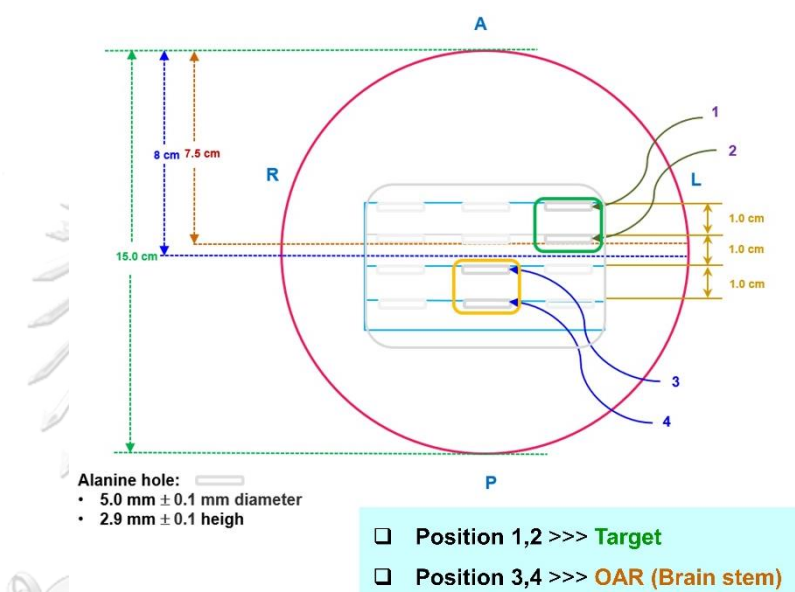


**Figure 3.20** The planned target volume (PTV), and the organs at risk (OAR)

- Then VMAT-SRS technique was used a beam size of 7×5 $cm^2$ for 6MV-FFF photon energy with the planned parameters as shown in Table 3.2 (17, 34).

**Table 3.2** Planned parameters.

| Parameter | Setting |
|---|---|
| Treatment technique | VMAT |
| Photon energy | 6MV-FFF |
| Prescribed dose (PTV) | 1800 cGy |
| Tolerance dose limits | |
| - Brain stem (OAR) | $D_{0.1\,cc} < 800$ cGy |

PTV: Planned target volume, OAR: Organ at risk,

VMAT: Volumetric modulated arc therapy,

MV-FFF: MV flattening filter free.

- All simulated plans were optimized with a dose of 1800 cGy in a single fraction. The parameters were optimized according to the following Table 3.3.

Table 3.3 Optimized parameters.

| ID/Type | Vol (%) | Dose (cGy) | Priority |
|---------|---------|------------|----------|
| PTV |  |  |  |
| Lower | 100.0 | 1800 | 300 |
| Upper | 0.0 | 1900 | 285 |
| OAR |  |  |  |
| Upper |  | 400 | 285 |

- The anisotropic analytical algorithm (AAA) was used to calculate the dose and plans were normalized to deliver 100 percent of the prescribed dose to 95 percent of the PTV volume.
- Following the above, the alanine pellets were placed in a fabricated head phantom and irradiated according to the plan.
- The three plans were analyzed by the cumulative dose-volume histogram (DVH) and tolerance limits as shown in Table 3.2.
- Finally, the results were analyzed.

## 3.10 Variable measurement

### 3.10.1 Independent variables

Independent variables include the type of treatment machine, treatment planning system, technique, dose calculation algorithm, dosimeter, and phantom.

### 3.10.2 Dependent variable

Dependent variable is the dose accuracy.

### 3.11  Statistical analysis

Mean, standard deviation, percentage dose difference, and uncertainty propagation were used for the analysis employing the Microsoft Excel program. The percentage dose difference was used to compare the output survey in each institution.

### 3.12  Expected benefits

3.12.1 Dose accuracy of SRS VMAT plans end-to-end test.

3.12.2 Conduction of the end-to-end test of SRS VMAT plans using an alanine dosimeter.

3.12.3 Alanine dosimeter can be applied in radiotherapy levels in the range of 1-20 Gy.

### 3.13  Outcome measurement

### 3.13.1 Section I: Optimization of EPR operation parameter

Optimization of EPR parameters

### 3.13.2 Section II: Alanine characteristics

Characteristics of alanine dosimeter and uncertainty of alanine

### 3.13.3 Section III: Output survey

Dose accuracy (%)

### 3.13.4 Section IV: End-to-end phantom fabrication and validation

Validated fabricated head phantom for end-to-end test.

### 3.14  Ethical consideration

According to the Belmont Report, this study respects the principle of beneficence/non-maleficence and justice for a person. This study was performed in a solid water phantom and fabricated head phantom. The research proposal has been submitted for approval to the Ethics Committee of Faculty of Medicine Chulalongkorn University in Bangkok, Thailand. The copy of the certificate of approval from the Institutional Review Board (IRB) is provided in Figure 3.21.

COE No. 022/2022

IRB No. 0345/65

INSTITUTIONAL REVIEW BOARD

Faculty of Medicine, Chulalongkorn University

1873 Rama IV Road, Patumwan, Bangkok 10330, Thailand, Tel 662-256-4493

Certificate of Exemption

(COE No. 022/2022)

The Institutional Review Board of the Faculty of Medicine, Chulalongkorn University, Bangkok, Thailand, has exempted the following study in compliance with the International guidelines for human research protection as Declaration of Helsinki, The Belmont Report, CIOMS Guideline, International Conference on Harmonization in Good Clinical Practice (ICH-GCP) and 45CFR 46.101(b)

Study Title :     Development of end-to-end test phantom for stereotactic radiosurgery using alanine dosimeter

Principal Investigator :   Miss Aungsumalin Intang

Study Center :     Department of Radiology, Faculty of Medicine, Chulalongkorn University.

Signature :  _____  Signature :  _____

(Emeritus Professor Tada Sueblinvong MD)     (Assistant Professor Thananya Thongtan PhD)

Chairperson     Member and Secretary

The Institutional Review Board     The Institutional Review Board

Date of Exemption :     May 18, 2022

Note   1. Continuing review report is not required.

2. Any changes or modifications of the exempted research proposal, required the submission of amendments to Med Chula IRB.

3. Final report is required after completion.

**Figure  3.21** The certificate of approval from the Ethics Committee of the Faculty of Medicine Chulalongkorn University.

CHAPTER 4

RESEARCH QUESTION AND RESEARCH OBJECTIVE

## 4.1 Section I: Optimization of EPR operation parameter

### 4.1.1 Microwave power (MP) and Modulation amplitude (MA)

Optimal MP was determined by plotting a graph between $MP^{1/2}$ setting and EPR intensity, as shown in Figure 4.1. Initially, the Intensity grows linearly as $MP^{1/2}$ increases and has the maximum $MP^{1/2}$ value of approximately 1.26. The graph then displays a peak form. For alanine readout of 100-2000 cGy subjected to 6MV-FFF linac, the maximum $MP^{1/2}$ value of 1.26 represents the optimal MP at 1.589 mW. Meanwhile, the optimal MA can be determined with the same condition. Figure 4.2 displays the relationship between MA and EPR intensity, where EPR increases as MA increases. The linear trend came to a halt at 7.018, and the optimal MA was determined at 7.018 G. Therefore, for the alanine dosimeter readout at dose of 100-2000 cGy subjected to 6MV-FFF linac, the optimal MP and MA in EPR is 1.589 mW and 7.018 G, respectively. The experimental results are shown in Appendix I.
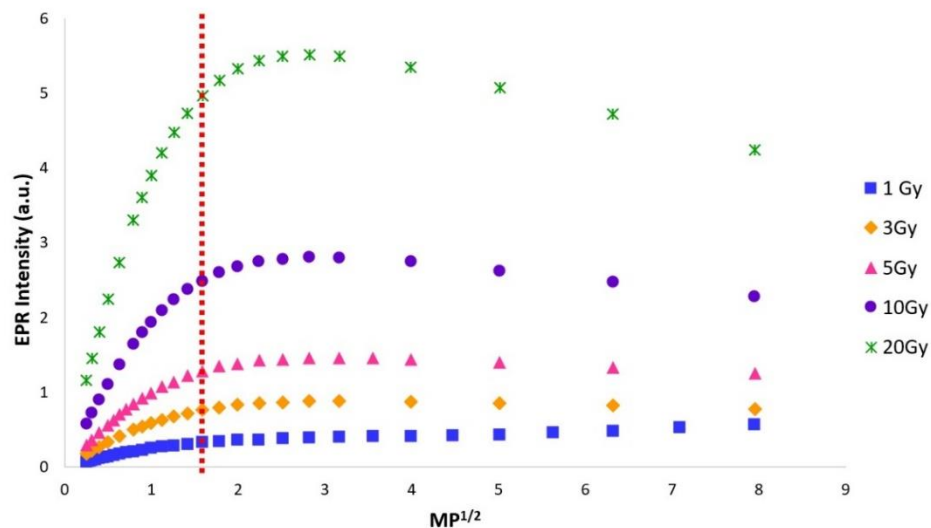


**Figure 4.1** Relationship between $MP^{1/2}$ setting and EPR intensity. Red line represents the maximum value of the linear $MP^{1/2}$ for an alanine readout of 100-2000 cGy subjected to a 6MV-FFF linac.
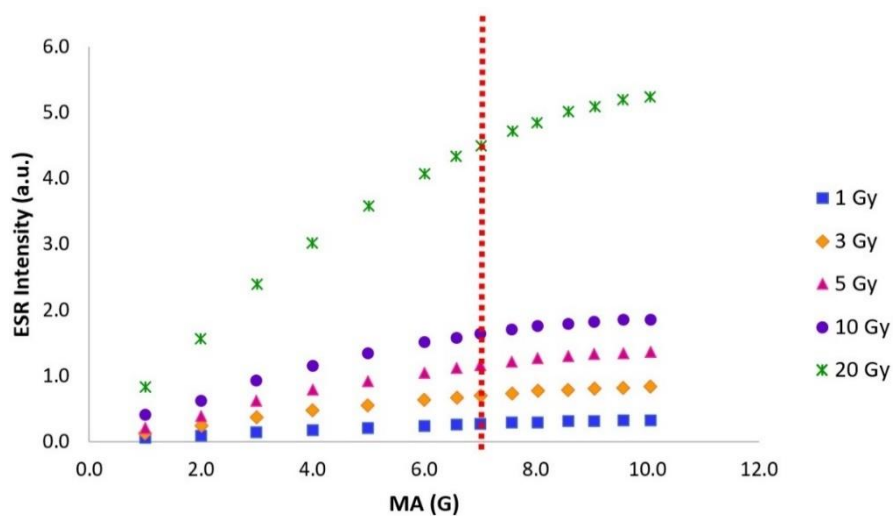
**Figure 4.2** Relationship between MA setting and EPR intensity. Red line represents the maximum value of the linear MA for an alanine readout of 100-2000 cGy subjected to a 6MV-FFF linac.

### 4.1.2 Time constant (TC)

Table 4.1 shows peak-to-peak width or $\Delta$Bpp and relative intensity (normalized to TC at 0.01 msec), where $\Delta$Bpp represents a high intensity of signal and relative intensity shows the resolution. With TC ranging from 0.01 to 5342.88 msec, both values are not significantly different. The optimal TC was determined at 40.96 msec in order to achieve high intensity and higher resolution.

**Table 4.1** The time constant on resolution and intensity of the spectra for 100-2000 cGy.

| Time constant (ms) | $\Delta$BPP (G)* | Relative intensity |
|---|---|---|
| 0.01 | 10.014 | 1.000 |
| 0.02 | 10.049 | 0.998 |
| 0.04 | 10.049 | 1.002 |
| 0.08 | 10.049 | 0.997 |
| 0.16 | 10.049 | 1.000 |
| 0.32 | 10.049 | 1.003 |

**Table 4.1 (Con't)** The time constant on resolution and intensity of the spectra for 100-2000 cGy.

| Time constant (ms) | $\Delta$BPP (G)* | Relative intensity |
|:---:|:---:|:---:|
| 0.64 | 10.049 | 0.999 |
| 1.28 | 10.154 | 1.001 |
| 2.56 | 10.183 | 1.001 |
| 5.12 | 10.049 | 0.996 |
| 10.24 | 10.049 | 0.998 |
| 20.48 | 10.049 | 0.999 |
| 40.96 | 10.719 | 0.996 |
| 81.92 | 10.173 | 0.998 |
| 163.84 | 10.052 | 0.988 |
| 327.68 | 10.479 | 0.974 |
| 655.36 | 11.388 | 0.908 |
| 1310.72 | 12.460 | 0.740 |
| 2521.44 | 13.815 | 0.558 |
| 5242.88 | 16.144 | 0.574 |

Note: $\Delta$BPP (G)*: the peak-to-peak width

## 4.2 Section II: Alanine characteristics

Measurements were conducted for seven characteristics, namely uniformity, reproducibility, linearity, repetition rate, energy dependence, directional dependence, and fading. The data was employed to estimate the uncertainty of alanine.

### 4.2.1 Uniformity and reproducibility of alanine dosimeter

Uniformity of the alanine dosimeter was explored in 10 alanine dosimeters as shown in Figure 4.3. The uniformity of alanine was considered by the standard deviation over 10 dosimeters and reported as ±0.22%. The error bars present the average standard deviation of five measurements for each alanine dosimeter. The reproducibility of this study revealed that the CV percentage was 1.16%.
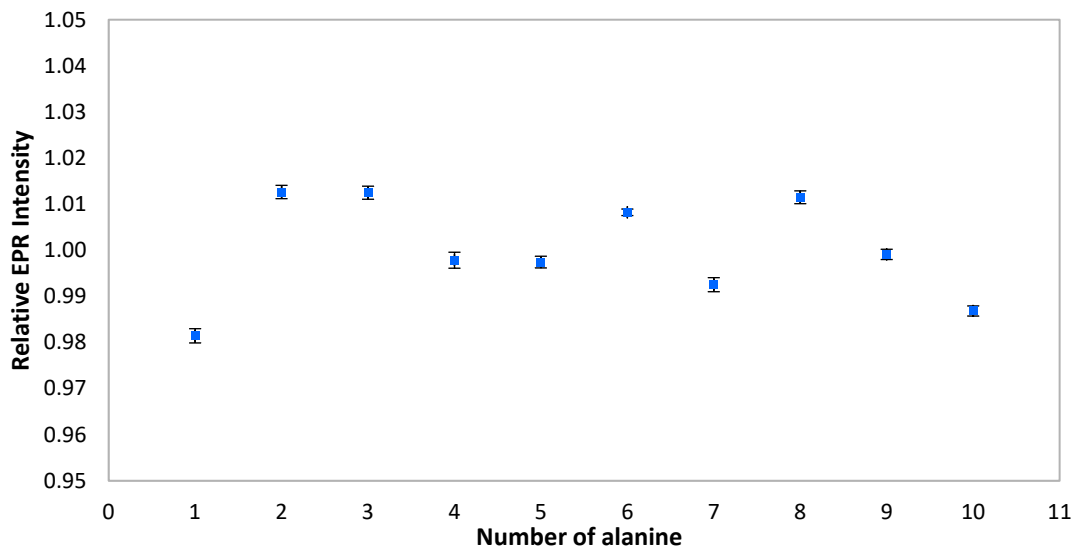
**Figure 4.3** Uniformity of 10 alanine for 6MV-FFF. The readout of alanine dosimeters was normalized to the average of 10 alanine dosimeters. Error bars show the standard deviation of 5 repeats.

### 4.2.2 Linearity

The increase in dose-response signal value was correlated to the radiation dose as shown in Figure 4.4. Following that, the EPR intensity and radiation dose were plotted. The response of the alanine dosimeter yielded a linear dose range from 0 to 3000 cGy presented the $R^2$ of 0.9998 and a linear equation obtained is y = 0.000585x + 0.0294.
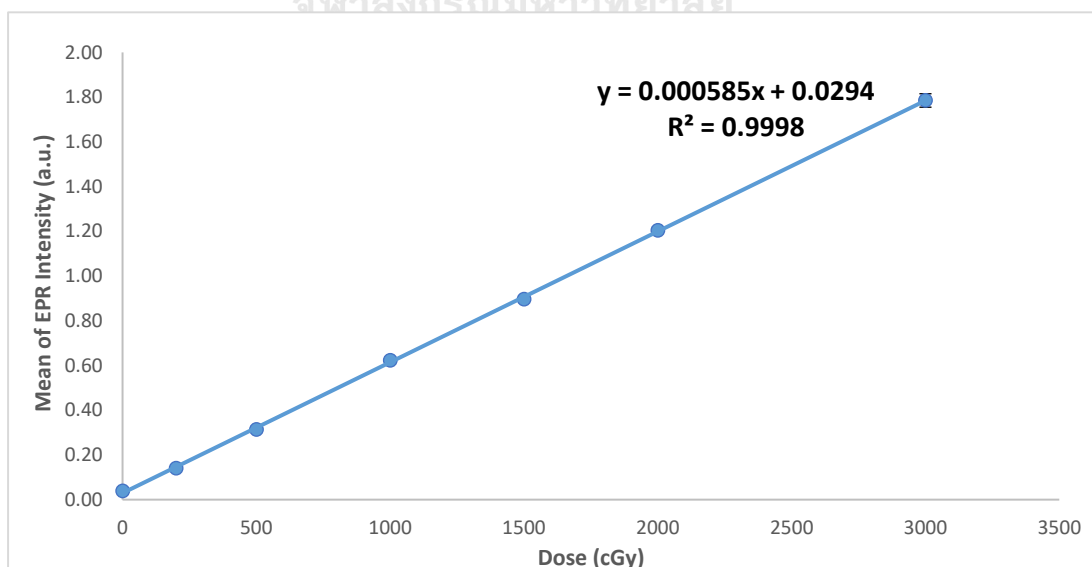


Figure 4.4 The linearity response of alanine dosimeter.

### 4.2.3 Repetition rate

The response of alanine dosimeter subjected to a varying repetition rate delivered by linac was investigated. Table 4.2 shows the results of the relative response by normalizing all repetition rates to 1400 MU/min. The deviation of repetition rate over 400 to 1400 MU/min is 0.80%.

Table 4.2 The repetition rate of the alanine dosimeter was normalized to 1400 MU/min.

| Repetition rate (MU/min) | Relative response to 1400 MU/min |
|---|---|
| 400 | 1.008 |
| 800 | 0.999 |
| 1200 | 0.998 |
| 1400 | 1.000 |

### 4.2.4 Energy dependence

The energy dependence of alanine dosimeter at 6 and 10 MV with and without flattening filter was investigated. Table 4.3 shows the relative result of beam energy with different filters, where $TPR_{20,10}$ is the IAEA TRS-398 photon beam quality index for megavoltage clinical photons produced by linac and relative response to 6MV-FFF. The maximum difference of relative response to 6MV-FFF is 0.80%

Table 4.3 Energy dependence of the alanine dosimeter from varied photon beams was normalized to 6MV-FFF.

| Photon beam | TPR 20,10 | Relative response to 6MV-FFF |
|---|---|---|
| 6MV-FFF | 0.63 | 1.000 |
| 6MV | 0.67 | 1.005 |
| 10MV-FFF | 0.71 | 0.997 |
| 10MV | 0.74 | 0.992 |

### 4.2.5 Directional dependence

The directional dependence of alanine dosimeter was tested in two directions, perpendicular and parallel to the beam axis, as indicated in Table 4.4. The result after normalization to the perpendicular side shows the difference of only 0.03%.

**Table 4.4** The directional dependence of the alanine dosimeter in two directions.

| Directional | Relative response |
|---|---|
| Perpendicular | 1.000 |
| Parallel | 0.997 |

### 4.2.6 Fading

The fading effect was examined for 12 consecutive weeks. As shown in Figure 4.5, the relative response to the first readout varies from 0.983 to 1.003. This fading over three months was 0.98%. This benefits in readout of alanine with low fading after long term storage. This study did not apply fading correction factors, the readout process was within two weeks after irradiation.
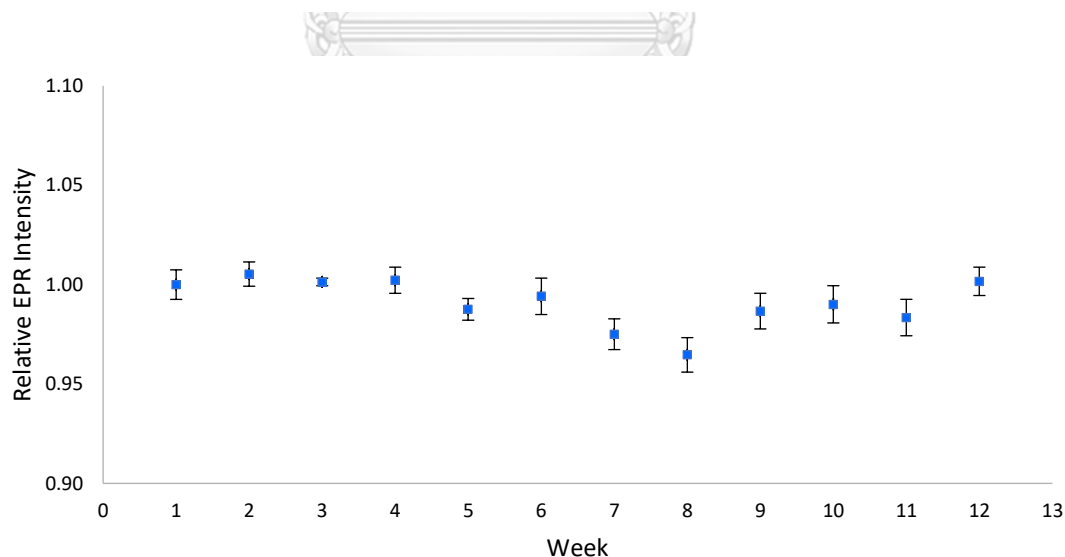


**Figure 4.5** Fading of alanine dosimeter over 12 weeks. Error bars represent standard deviation of relative response from 5 alanine dosimeters.

### 4.2.7 Uncertainty

The uncertainty of alanine dosimeter is presented in Table 4.5. The list of uncertainty sources comes from the alanine characteristics in this study, mechanical of Varian TrueBeam, and the mass of alanine (from the manufacturer). Overall, the expanded uncertainty is 2.68% at 95% confidence interval.

**Table 4.5** Uncertainty of alanine following "Guide to the expression of uncertainty in measurement"(29).

| Source of uncertainty | Type | U (%) |
|---|:---:|:---:|
| Uniformity | A | 0.37 |
| Reproducibility | A | 0.03 |
| Linearity | A | 0.45 |
| Energy response | A | 0.19 |
| Repetition rate | A | 0.19 |
| Fading | A | 0.10 |
| Directional | A | 0.36 |
| Alanine mass | B | 0.01 |
| Mechanical of machine | B | 0.50 |
| Calibration factor (ND,w) | B | 1.00 |
| Correction for irradiation Temperature | B | 0.00 |
| Combined uncertainty (Uc) | | 1.34 |
| Coverage factor (k) | | 2.0 |
| Expanded uncertainty | | 2.68 |

**4.3  Section III: Output measurement survey**

**4.3.1  Output measurement survey**
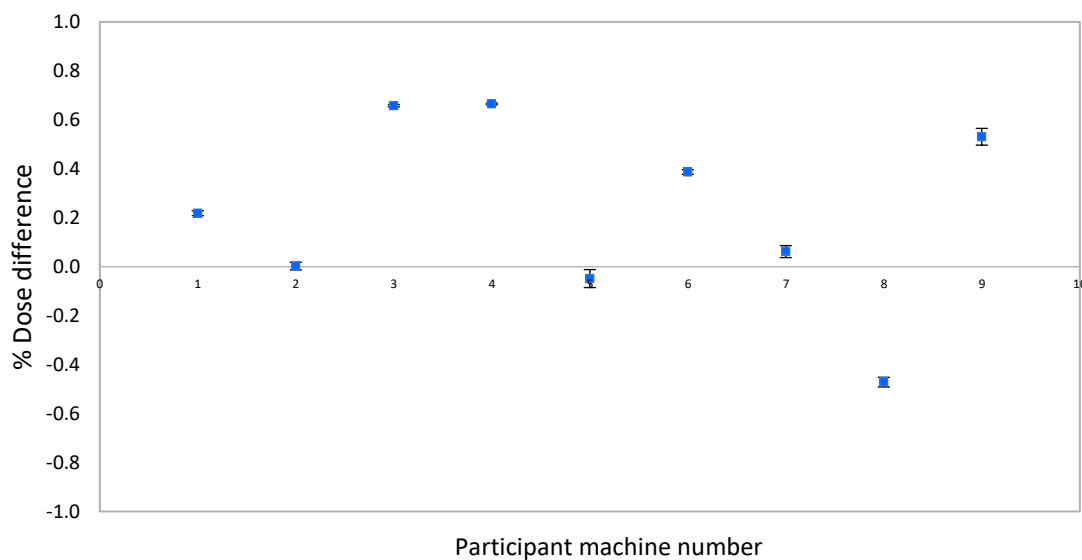


**Figure  4.6** The percent difference of output survey in each participant.

All  radiotherapy  centers  participating  in  this  study  calibrate  their  routine
dosimeters and validate the dose output on a regular basis. Therefore, all the results
can  be  traced  to  the  SI  unit  with  reliable  uncertainty,  assuring  that  the  delivered
dose  from  the  linac  machines  is  accurate.  Figure  4.6  depicts  the  output
measurement of 6MV-FFF at a dose of 10 Gy using alanine dosimeters from 9 distinct
linac  machines.  The  difference  of  output  is  within  ±1.0%.  The  overall  different
percentage  output  of  8  participants  was  within  ±2.2%  uncertainty  at  a  95%
confidence interval.

**4.4  Section IV: End-to-end phantom fabrication and validation**

**4.4.1  Fabrication of head phantom**

**4.4.1.1    Material and design of the fabricated head phantom**

The  head  phantom  was  designed  and  fabricated  according  to  the
drawings  as  shown  in  Figure  4.7.  The  phantom  was  designed  using  cast  nylon,
having  a  CT  number  of  approximately  80-100  HU  throughout  the  phantom.  As
seen  in  Figure  4.8,  the  result  shows  that  no  artifacts  and  no  significant
difference of dimensions between the phantom and the plane were found.
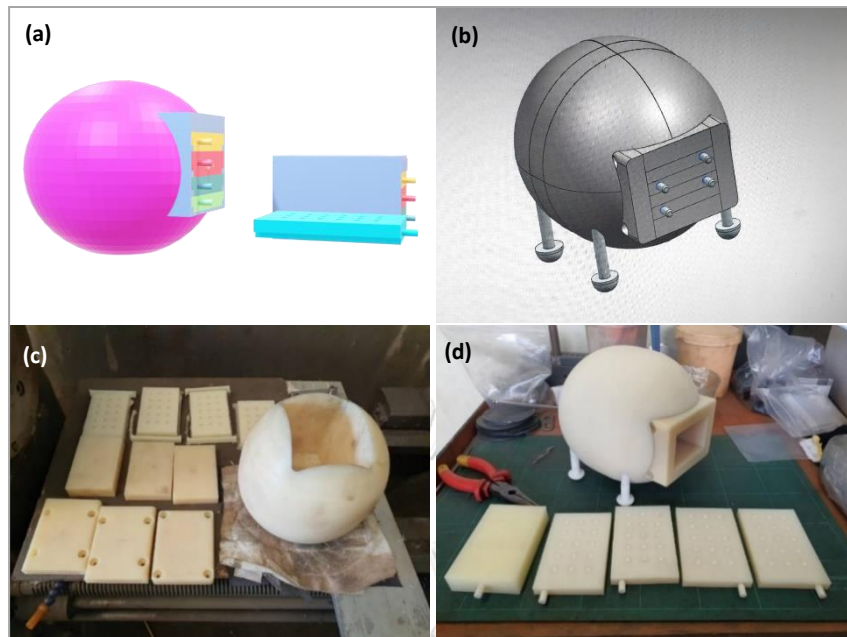
**Figure 4.7**: Fabricated cast nylon head phantom: (a) 3D head phantom design, different colors showing different parts of phantom component, (b) 3D head phantom design with four feet by CAD, (c) fabricated cast nylon head phantom parts using CNC technique, consisting of head drilled sphere for head phantom and alanine box set, and (d) a complete set of fabricated cast nylon head phantom.
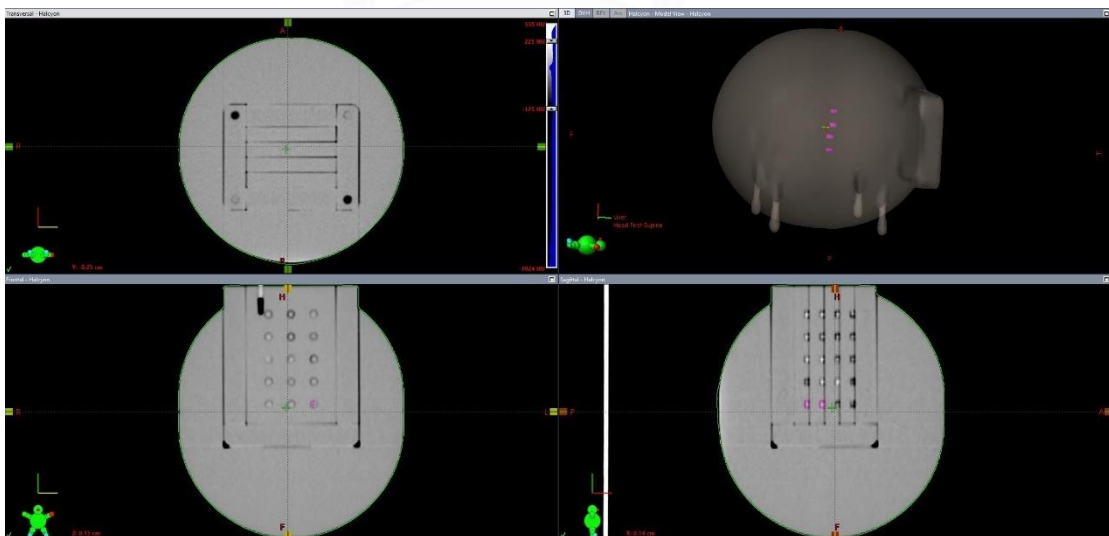


**Figure 4.8** CT images of the fabricated head phantom.

**4.4.2 Validation of the fabricated head phantom**

**4.4.2.1 End-to-end phantom validation**

The results of VMAT SRS plans are listed in Table 4.6. The Table indicates that the target percentage dose difference ranges from 0.01 to 1.16 for the fabricated cast nylon end-to-end test head phantom for TrueBeam. Despite the fact that the percentage dose difference range in the OAR was larger, ranging from 3.65 to 11.95 for TrueBeam. The mean of the three plans with the target percentage dose difference was -0.66±0.92 (mean±SD), while the mean of the three plans in OAR was -3.94±0.92.

**Table 4.6** Validation of the fabricated cast nylon end-to-end test head phantom (%Difference = $(D_{alanine} - D_{TPS})/D_{TPS}*100$). Positions 1 and 2 represent the target while positions 3 and 4 represent the brain stem.

| Plan No. | Position | TPS (cGy) | Alanine (cGy) (mean±SD) | %Difference |
|:---:|:---:|:---:|:---:|:---:|
| 1 | 1 | 1891.3±5.8 | 1906.5±20.0 | 0.80 |
| | 2 | 1880.0±4.8 | 1901.8±8.7 | 1.16 |
| | 3 | 181.4±19.7 | 197.7±2.9 | 8.99 |
| | 4 | 131.0±8.3 | 129.2±8.0 | −1 .40 |
| 2 | 1 | 1885.8±6.5 | 1908.6±14.3 | 1.21 |
| | 2 | 1867.6±8.4 | 1867.3±10.3 | −0.01 |
| | 3 | 187.3±17.8 | 196.2±1.7 | 4.73 |
| | 4 | 106.4±6.2 | 102.5±0.7 | −3.65 |

**Table 4.6 (Con't)** Validation of the fabricated cast nylon end-to-end test head phantom (%Difference = ($D_{alanine}$ − $D_{TPS}$ )/$D_{TPS}$*100). Positions 1 and 2 represent the target while positions 3 and 4 represent the brain stem.

| Plan No. | Position | TPS (cGy) | Alanine (cGy) (mean±SD) | %Difference |
|---|---|---|---|---|
| 3 | 1 | 1880.2±5.8 | 1892.9±21.0 | 0.67 |
| | 2 | 1892.4±5.5 | 1874.0±14.9 | −0.97 |
| | 3 | 182.6±21.5 | 204.4±4.8 | 11.95 |
| | 4 | 107.9±7.6 | 112.8±0.8 | 4.51 |
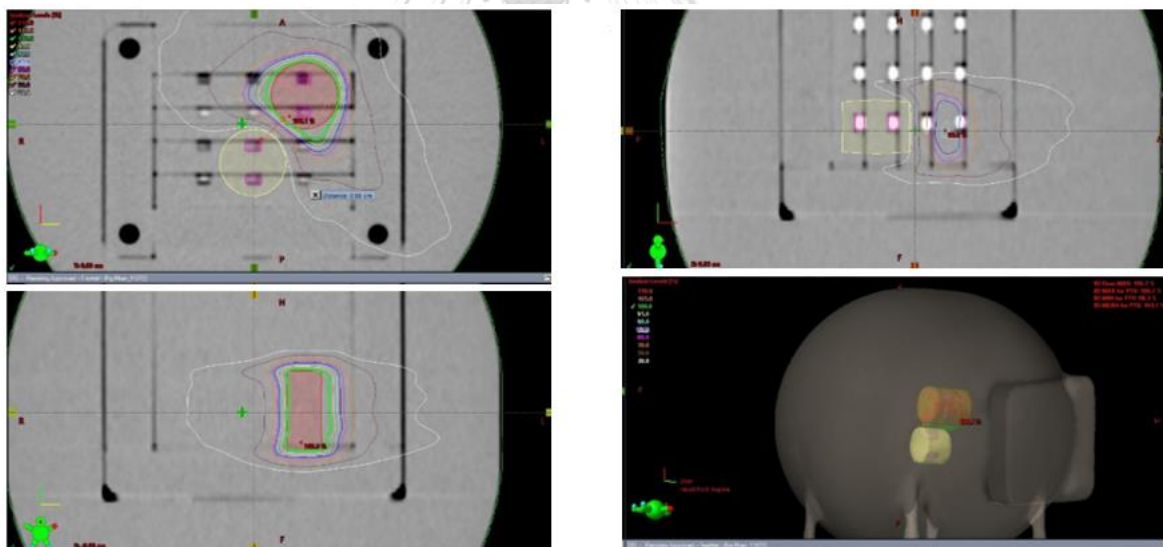


**Figure 4.9** Fabricated head phantom isodose distribution in axial, coronal, sagittal, and 3D view from VMAT from plan1.

Figure 4.9 shows the distance between the target (Position 2) and brainstem (Position 3) being 0.88 cm which is the closest distance between PTV and point of measurement in OAR. Figure 4.10 shows the dose profile of the fabricated head phantom. This maximum dose is 106.9%.

**Figure 4.10** The dose profile of the fabricated head phantom.

**Uncertainty budget**

The uncertainty of the End-to-End test is presented in Table 4.7. The uncertainty numbers 1 to 7 are the characteristics of alanine which have been obtained from the previous in-house study. The characteristic consists of uniformity, reproducibility, linearity, repetition rate, energy dependence, directional dependence, and fading. The standard output uncertainty was calculated from the mechanical QA process. The uncertainty of ionization chamber calibration was reported at 1% for absorbed dose to water which can be traced to SSDL Thailand. Overall, at 95% confidence interval (k=2), the expanded uncertainty of measurement was calculated to be 2.8%.

**Table 4.7** Uncertainty of alanine following "Guide to the expression of uncertainty in measurement" (29)

| No | Source of uncertainty | Type | Relative standard uncertainty (%) |
|----|----------------------|------|-----------------------------------|
| 1 | Uniformity of alanine dosimeter | A | 0.4 |
| 2 | Reproducibility of alanine dosimeter | A | 0.1 |
| 3 | Linearity of alanine dosimeter | A | 0.4 |
| 4 | Repetition rate of alanine dosimeter | A | 0.2 |

**Table 4.7** Uncertainty of alanine following "Guide to the expression of uncertainty in measurement"(29)

| No | Source of uncertainty | Type | Relative standard uncertainty (%) | |
|----|----------------------|------|-----------------------------------|---|
| 5 | Energy dependence of alanine dosimeter | A | 0.2 | |
| 6 | Directional of alanine dosimeter | A | 0.1 | |
| 7 | Fading of alanine dosimeter | A | 0.4 | |
| 8 | Standard output | B | 0.5 | |
| 9 | $N_{D,w}$ calibration of the user dosimeter at the standard laboratory | B | 1.0 | |
| | | Combined uncertainty (Uc) | | 1.4 |
| | | Coverage factor (k) | | 2.0 |
| | | **Expanded uncertainty** | | **2.8** |

จุฬาลงกรณ์มหาวิทยาลัย

CHULALONGKORN UNIVERSITY

## CHAPTER 5

## RESEARCH METHODOLOGY

### 5.1 Discussion

Several metrology institutions developed the alanine and EPR technique as a secondary standard for absorbed dose to water in the kGy dose range,(35-37) primarily for industrial applications. The spectrum acquisition parameter used for EPR can affect the quantitative determination of three parameters: microwave power (MP), modulation amplitude (MA), and time constant (TC) (22). Both MP and MA have an effect on the shape, resolution, and amplitude of the spectrum. Initially, sensitivity increases with an increase in MP or MA, and then decreases. The EPR amplitude is averaged at each spectrum point as the time constant is expanding, reducing the influence of background noise caused by electronic devices. Figures 4.1a and b demonstrate that the EPR response initially changes linearly with MA and the square root of MP, but then deviates from this linearity. This is due to the broadening of the peaks and changes in the shape of the spectra. Thus, the optimum MP and MA parameters in the EPR setting are 2 mW (attenuation to 21 dB) and 7.018 G, respectively. These findings are consistent with those of Garcia et al. (38) and Gago-Arias et al. (28).

The characteristics of the alanine dosimeter was examined in 6MV-FFF for the uniformity of alanine by the standard deviation over 10 dosimeters and reported as ±0.22%. This demonstrates that the alanine dosimeter has high uniformity within the same batch. The reproducibility of this study revealed that the CV percentage was 1.16%, indicating that the EPR system was very stable. Furthermore, Figure 4.3 shows that the EPR Intensity demonstrated a linear proportion to the dose from 0 to 3000 cGy ($R^2$ = 0.9998). This value agreed with the findings of Mansour (2018) (15) and Garcia et al. (2009) (38). This contributes to the feasibility of using alanine dosimeters in radiotherapy dose range (1-20 Gy). Additionally, the deviation of repetition rate over 400 to 1400 MU/min in Table 4.2 is 0.80%, indicating that the high repetition rate had no effect on the readout of the alanine dosimeter. Table 4.3 shows that the

maximum difference of relative response to 6MV-FFF is 0.80%, which is consistent with the energy dependence reported by Mansour (15). It demonstrated that the high repetition rate had no effect on the readout of the alanine dosimeter and indicated that the dosimeter is energy independent. For angular dependence, Table 4.4 shows that the difference after normalizing to the perpendicular side is only 0.03%. This confirms that the irradiation angular had no effect on the alanine dosimeter. Furthermore, the fading effect was examined for 12 consecutive weeks. As seen in Figure 5, the relative response to the first readout varied from 0.983 to 1.003. This fading over three months was 0.98%, but Zeng GG et al. (39) reported 5% in a single year. This study did not apply fading correction factors, and the readout process was within two weeks after irradiation. Overall, the expanded uncertainty was 2.68% at 95% confidence interval. A previous investigation by Mansour (16) reported an uncertainty of 1.52% for 10 Gy, and Garcia et al. (38) reported an uncertainty of 4.9% for 2 Gy and 1.4% for 10 Gy. In the dose range 2-10 Gy, the higher extended uncertainty of 4.9% (k= 2) has been evaluated, implying that the alanine/ESR dosimetry system may be applied to the radiotherapy dose level that demands a worldwide accuracy of 5% (ICRU24,1976) (40).

All radiotherapy centers participating in this study calibrate their routine dosimeters and validate the dose output on a regular basis. With reliable uncertainty, all findings can be traced to the SI unit. This assures the accuracy of the delivered dose from the linear accelerator machines. Figure 4.6 illustrates the output measurement of 6MV-FFF using alanine dosimeters from nine different linear accelerator machines at a dose of 1000 cGy. The difference between outputs is within ±1.0%, contributing to the practicality of using the alanine dosimeter in quality audit programs and interlaboratory comparison.

As shown in Figure 4.8, the fabricated cast nylon end-to-end test head phantom was presented as a homogeneous material with no artifacts and a CT number about 80-100 HU. According to Table 4.6, the target percentage dose difference for the fabricated cast nylon end-to-end test head phantom for three plans TrueBeam ranges from 0.01 to 1.71, despite the fact that the percentage difference in OAR for TrueBeam ranged from 0.84 to 10.67. Dimitriadis et al. (2017)

(23) reported 18.76% with 1.2% agreement between plastic scintillation detector (PSD) and a pellet alanine in the OAR. Since the measurement was conducted in a high dose gradient area, the distance between the target (Position 2) and brainstem (Position 3) was 0.88 cm (Figure 4.9), it is the distance between the planning target volume (PTV) and OAR, or Position 2 and Position 3, which is the closest distance between PTV and point of measurement in OAR. The differences between treatment planning system (TPS) calculated doses are larger in the OAR than in the target, during A high variation of dose was found in Position 3 of TPS were SD=19.7, 17.8 and 21.5 in plan 1, plan 2 and plan 3, respectively. This contributes to a large dose difference when low dose at brainstem were performed.

The lack of a skull in the fabricated head phantom is a limitation of this study. Furthermore, the measurement was not performed suitably in a high dose gradient area. This variation might be due to the size of the alanine dosimeters being 4.8±0.1 mm in diameter and 2.8±0.1 mm in height. Hence, an alanine dosimeter slide should be fabricated into a small passive dosimeter, such as a radiophotoluminescent glass dosimeter has a diameter of 1.5 mm for further investigation.

## 5.2 Conclusions

This study determined the optimal EPR operation key parameters for alanine dosimeter readout subjected to 6MV in doses ranging from 1-2000 cGy, which is often applied in radiotherapy. To maintain better resolution and higher intensity of the spectrum, the EPR operation parameters of alanine dosimeters for radiotherapy were adjusted to MP of 2 mW (attenuation to 21 dB), MA of 7.018 G, and TC of 40.96 ms. Both key parameters (MA and TC) are consistent with the previous reports, while only MP is slightly different which may be attributable to human error.

In addition, characteristics of the alanine dosimeter have been investigated. From the resulting percent difference of output survey in each participatory radiotherapy center, this dosimeter is a potential alternative transfer dosimeter in quality control, postal audit, and intercomparison. The dosimeter has demonstrated a good radiation response in doses of 1-2000 cGy, which is significantly lower than its general application (kGy), good uniformity, linearity response, angle and energy

independence, low fading, and the uncertainty of measurement of 2.68%. The dose output comparison between nine linear accelerator machines (from 8 radiotherapy centers) revealed that the difference in results measured by alanine dosimeter is within ±1.0%, increasing the potential for postal audit.

This study presented the development of a novel fabricated cast nylon end-to-end test head phantom suitably designed to image and irradiate during an end-to-end test for stereotactic radiosurgery using alanine dosimeter. Moreover, this fabricated cast nylon head phantom is a multifunctional and cost-effective tool for dosimetric verification of radiotherapy treatment planning systems that shall benefit various radiotherapy institutes.

# REFERENCES

1.      Poder J, Brown R, Porter H, Gupta R, Ralston A. Development of a dedicated phantom for multi‑target single‑isocentre stereotactic radiosurgery end to end testing. Journal of applied clinical medical physics. 2018;19(6):99-108.

2.      Izewska J, Andreo P. The IAEA/WHO TLD postal programme for radiotherapy hospitals. Radiotherapy and oncology. 2000;54(1):65-72.

3.      Izewska J, Andreo P, Vatnitsky S, Shortt KR. The IAEA/WHO TLD postal dose quality audits for radiotherapy: a perspective of dosimetry practices at hospitals in developing countries. Radiotherapy and oncology. 2003;69(1):91-7.

4.      Ibbott GS, Followill DS, Molineu HA, Lowenstein JR, Alvarez PE, Roll JE. Challenges in credentialing institutions and participants in advanced technology multi-institutional clinical trials. International Journal of Radiation Oncology* Biology* Physics. 2008;71(1):S71-S5.

5.      Molineu A, Followill DS, Balter PA, Hanson WF, Gillin MT, Huq MS, et al. Design and implementation of an anthropomorphic quality assurance phantom for intensity-modulated radiation therapy for the Radiation Therapy Oncology Group. International Journal of Radiation Oncology* Biology* Physics. 2005;63(2):577-83.

6.      Taylor ML, Kron T, Franich RD. A contemporary review of stereotactic radiotherapy: inherent dosimetric complexities and the potential for detriment. Acta oncologica. 2011;50(4):483-508.

7.      Faught AM, Kry SF, Luo D, Molineu A, Bellezza D, Gerber RL, et al. Development of a modified head and neck quality assurance phantom for use in stereotactic radiosurgery trials. Journal of applied clinical medical physics. 2013;14(4):206-15.

8.      Kron T, Haworth A, Williams I, editors. Dosimetry for audit and clinical trials: challenges and requirements. Journal of Physics: Conference Series; 2013: IOP Publishing.

9.      Iżewska J, Georg D, Bera P, Thwaites D, Arib M, Saravi M, et al. A methodology for TLD postal dosimetry audit of high-energy radiotherapy photon beams in non-reference conditions. Radiotherapy and oncology. 2007;84(1):67-74.

10.     Kroutilíková D, Novotný J, Judas L. Thermoluminescent dosimeters (TLD) quality assurance network in the Czech Republic. Radiotherapy and oncology. 2003;66(2):235-44.

11.     Mizuno H, Kanai T, Kusano Y, Ko S, Ono M, Fukumura A, et al. Feasibility study of glass dosimeter postal dosimetry audit of high-energy radiotherapy photon beams. Radiotherapy and Oncology. 2008;86(2):258-63.

12.     Lye J, Dunn L, Kenny J, Lehmann J, Kron T, Oliver C, et al. Remote auditing of radiotherapy facilities using optically stimulated luminescence dosimeters. Medical physics. 2014;41(3):032102.

13.     Pulliam KB, Followill D, Court L, Dong L, Gillin M, Prado K, et al. A six-year review of more than 13,000 patient-specific IMRT QA results from 13 different treatment sites. Journal of applied clinical medical physics. 2014;15(5):196-206.

14.     Clark CH, Aird EG, Bolton S, Miles EA, Nisbet A, Snaith JA, et al. Radiotherapy dosimetry audit: three decades of improving standards and accuracy in UK clinical practice and trials. The British journal of radiology. 2015;88(1055):20150251.

15.     Mansour I. Development of mailed dosimetric audit for external beam radiation therapy using alanine dosimeters: Carleton University; 2018.

16.     Kaluska I, Gluszewski W. Materials of the Regional Training Course on Validation and Process Control for Electron Beam Radiation Processing. 2007.

17.     Buatti JM, Friedman WA, Meeks SL, Bova FJ. RTOG 90-05: the real conclusion. International journal of radiation oncology, biology, physics. 2000;47(2):269-71.

18.     Schulz R, Maryanski M, Ibbott G, Bond J. Assessment of the accuracy of stereotactic radiosurgery using Fricke-infused gels and MRI. Medical physics. 1993;20(6):1731-4.

19.     Coscia G, Vaccara E, Corvisiero R, Cavazzani P, Ruggieri FG, Taccini G. Fractionated stereotactic radiotherapy: a method to evaluate geometric and dosimetric uncertainties using radiochromic films. Medical physics. 2009;36(7):2870-80.

20.     Seravalli E, Van Haaren P, Van Der Toorn P, Hurkmans C. A comprehensive evaluation of treatment accuracy, including end-to-end tests and clinical data, applied to intracranial stereotactic radiotherapy. Radiotherapy and Oncology. 2015;116(1):131-8.

21.    RT W. Xenon User's Guide. Billerica, MA USA: Bruker BioSpin Corporation; 2012.

22.    Goodman BA, Worasith N, Ninlaphruk S, Mungpayaban H, Deng W. Radiation Dosimetry Using Alanine and Electron Paramagnetic Resonance (EPR) Spectroscopy: A New Look at an Old Topic. Applied Magnetic Resonance. 2017;48:155-73.

23.    Dimitriadis A, Palmer AL, Thomas RA, Nisbet A, Clark CH. Adaptation and validation of a commercial head phantom for cranial radiosurgery dosimetry end-to-end audit. The British Journal of Radiology. 2017;90(1074):20170053.

24.    Loughery B, Knill C, Silverstein E, Zakjevskii V, Masi K, Covington E, et al. Multi-institutional evaluation of end-to-end protocol for IMRT/VMAT treatment chains utilizing conventional linacs. Medical Dosimetry. 2019;44(1):61-6.

25.    Wesolowska P, Georg D, Lechner W, Kazantsev P, Bokulic T, Tedgren AC, et al. Testing the methodology for a dosimetric end-to-end audit of IMRT/VMAT: results of IAEA multicentre and national studies. Acta Oncologica. 2019;58(12):1731-9.

26.    Sookpeng S, Cheebsumon P, Pengpan T, Martin C. Comparison of computed tomography dose index in polymethyl methacrylate and nylon dosimetry phantoms. Journal of Medical Physics/Association of Medical Physicists of India. 2016;41(1):45.

27.    Sharpe PH, Sephton JP. Alanine dosimetry at NPL-the development of a mailed reference dosimetry service at radiotherapy dose levels. 1998.

28.    Gago-Arias A, González-Castaño D, Gómez F, Peteiro E, Lodeiro C, Pardo-Montero J. Development of an alanine dosimetry system for radiation dose measurements in the radiotherapy range. Journal of Instrumentation. 2015;10(08):T08004.

29.    organizations Jm. Evaluation of measurement data — Guide to the expression of uncertainty in measurement. JCGM 100: JCGM; 2008.

30.    Kamomae T, Shimizu H, Nakaya T, Okudaira K, Aoyama T, Oguchi H, et al. Three-dimensional printer-generated patient-specific phantom for artificial in vivo dosimetry in radiotherapy quality assurance. Physica medica. 2017;44:205-11.

31.    Kadoya N, Abe K, Nemoto H, Sato K, Ieko Y, Ito K, et al. Evaluation of a 3D-printed heterogeneous anthropomorphic head and neck phantom for patient-specific quality assurance in intensity-modulated radiation therapy. Radiological Physics and Technology. 2019;12:351-6.

32.    Alshipli M, Kabir NA, Hashim R, Marashdeh M. Measurement of attenuation coefficients and CT numbers of epoxy resin and epoxy-based Rhizophora spp particleboards in computed tomography energy range. Radiation Physics and Chemistry. 2018;149:41-8.

33.    Solc J, Vrba T, Burianova L. Tissue-equivalence of 3D-printed plastics for medical phantoms in radiology. Journal of Instrumentation. 2018;13(09):P09018.

34.    Milano MT, Usuki KY, Walter KA, Clark D, Schell MC. Stereotactic radiosurgery and hypofractionated stereotactic radiotherapy: normal tissue dose constraints of the central nervous system. Cancer treatment reviews. 2011;37(7):567-78.

35.    McLaughlin WL, Desrosiers MF. Dosimetry systems for radiation processing. Radiation Physics and Chemistry. 1995;46(4-6):1163-74.

36.    Regulla D, Deffner U. Dosimetry by ESR spectroscopy of alanine. The International Journal of Applied Radiation and Isotopes. 1982;33(11):1101-14.

37.    Sharpe P, Rajendran K, Sephton J. Progress towards an alanine/ESR therapy level reference dosimetry service at NPL. Applied Radiation and Isotopes. 1996;47(11-12):1171-5.

38.    Garcia T, Lin M, Pasquié I, Lourenço V. A methodology for choosing parameters for ESR readout of alanine dosimeters for radiotherapy. Radiation Physics and Chemistry. 2009;78(9):782-90.

39.    Zeng G, McEwen M, Rogers D, Klassen N. An experimental and Monte Carlo investigation of the energy dependence of alanine/EPR dosimetry: I. Clinical x-ray beams. Physics in Medicine & Biology. 2004;49(2):257.

40.    (ICRU) ICoruam. Determination of absorbed dose in a patient irradiated by beams of X and Gamma rays in radiotherapy procedures. Washington DC1976.

## APPENDIX I
## The results of Microwave power (MP), Modulation amplitude (MA) and
## Time constant (TC)

The selection of the spectrum acquisition parameter for EPR can influence the quantitative determination of three parameters: microwave power (MP), modulation amplitude (MA), and time constant (TC). EPR sensitivity often increases with increasing MP and MA. For a clear signal, MP was investigated first, followed by MA and TC. The MP value obtained from the first step was used to investigate MA. Moreover, the other acquisition parameters were set as follows:

- center field: 3500 G
- sweep width: 200 G
- modulation frequency: 100 kHz
- sweep time: 40.45 s
- receiver gain: 30 dB
- number of scans: 3 time

**Microwave power (MP)** was used as an acquisition parameter as described above, MA was set to 7.018 G according to the previous study (28)(29) and TC was set to a minimum of 0.01 msec.(28)(9) Following that, MP was changed from minimum to maximum (5 to 35 dB, increasing 1 dB in each step) and the acquisition parameters were used at doses 100, 200, 500, 1000, and 2000 cGy, as listed in Table I.1. Figure I.1 shows the EPR spectra of irradiated dose at 100, 200, 500, 1000, and 2000 cGy alanine with MP value of 1.589 mW, where all spectra were collected with modulation amplitude of 7.018 G and sweep time of 40.45 s.

Table I.1 The result of microwave power (MP) was fixed at MA=7.018 G, while MP was attenuated one step from 5 to 35 dB and all other parameters were adjusted as described above.

| Attenuation (dB) | MP (mW) | Dose SQRT(MP) | 100 cGy Height | 300 cGy Height | 500 cGy Height | 1000 cGy Height | 2000 cGy Height |
|---|---|---|---|---|---|---|---|
| 35 | 0.06325 | 0.2515 | 0.0697 | 0.1719 | 0.2957 | 0.5794 | 1.1599 |
| 34 | 0.0796 | 0.2822 | 0.0819 | | | | |
| 33 | 0.1002 | 0.3165 | 0.0912 | 0.2160 | 0.3678 | 0.7230 | 1.4589 |
| 32 | 0.1262 | 0.3552 | 0.0987 | | | | |
| 31 | 0.1589 | 0.3986 | 0.1103 | 0.2691 | 0.4588 | 0.8972 | 1.8077 |
| 30 | 0.2000 | 0.4472 | 0.1238 | | | | |
| 29 | 0.2518 | 0.5018 | 0.1384 | 0.3318 | 0.5658 | 1.1091 | 2.2428 |
| 28 | 0.3170 | 0.5630 | 0.1563 | | 0.6294 | | |
| 27 | 0.3991 | 0.6317 | 0.1744 | 0.4059 | 0.6974 | 1.3634 | 2.7372 |
| 26 | 0.5024 | 0.7088 | 0.1882 | | 0.7696 | | |
| 25 | 0.6325 | 0.7953 | 0.2053 | 0.4990 | 0.8391 | 1.6389 | 3.2992 |
| 24 | 0.7962 | 0.8923 | 0.2263 | 0.5411 | 0.9216 | 1.7962 | 3.6057 |
| 23 | 1.0020 | 1.0010 | 0.2492 | 0.5914 | 0.9937 | 1.9382 | 3.8976 |
| 22 | 1.2620 | 1.1234 | 0.2684 | 0.6333 | 1.0768 | 2.0894 | 4.1971 |
| 21 | 1.5890 | 1.2606 | 0.2861 | 0.6796 | 1.1427 | 2.2340 | 4.4774 |
| 20 | 2.0000 | 1.4142 | 0.3079 | 0.7211 | 1.2268 | 2.3783 | 4.7392 |
| 19 | 2.5180 | 1.5868 | 0.3331 | 0.7617 | 1.2840 | 2.4909 | 4.9704 |
| 18 | 3.1700 | 1.7804 | 0.3461 | 0.7982 | 1.3462 | 2.6037 | 5.1718 |
| 17 | 3.9910 | 1.9977 | 0.3641 | 0.8316 | 1.3868 | 2.6807 | 5.3281 |
| 16 | 5.0240 | 2.2414 | 0.3667 | 0.8544 | 1.4283 | 2.7448 | 5.4331 |
| 15 | 6.3250 | 2.5150 | 0.3809 | 0.8645 | 1.4428 | 2.7774 | 5.4911 |
| 14 | 7.9620 | 2.8217 | 0.3931 | 0.8798 | 1.4563 | 2.8031 | 5.5087 |
| 13 | 10.0200 | 3.1654 | 0.3960 | 0.8822 | 1.4624 | 2.7942 | 5.4931 |
| 12 | 12.6200 | 3.5525 | 0.4052 | | 1.4590 | | |
| 11 | 15.8900 | 3.9862 | 0.4061 | 0.8771 | 1.4447 | 2.7420 | 5.3520 |

**Table I.1 (Con't)** The result of microwave power (MP) was fixed at MA=7.018 G, while MP was attenuated one step from 5 to 35 dB and all other parameters were adjusted as described above.

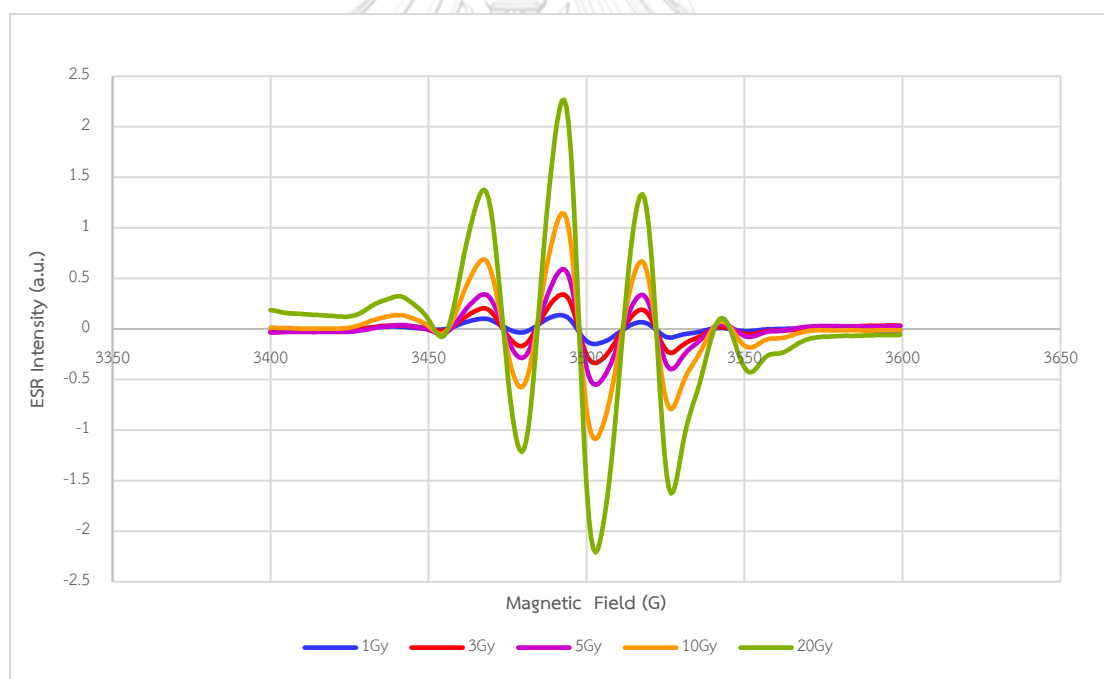| Attenuation | MP | Dose | EPR Intensity | | | | |
|---|---|---|---|---|---|---|---|
| (dB) | (mW) | SQRT(MP) | 100 cGy | 300 cGy | 500 cGy | 1000 cGy | 2000 cGy |
| 10 | 20.0000 | 4.4721 | 0.4246 | | | | |
| 9 | 25.1800 | 5.0180 | 0.4311 | 0.8543 | 1.3977 | 2.6295 | 5.0743 |
| 8 | 31.7000 | 5.6303 | 0.4601 | | | | |
| 7 | 39.9100 | 6.3174 | 0.4753 | 0.8234 | 1.3354 | 2.4756 | 4.7172 |
| 6 | 50.2400 | 7.0880 | 0.5326 | | | | |
| 5 | 63.2500 | 7.9530 | 0.5600 | 0.7790 | 1.2542 | 2.2780 | 4.2472 |



**Figure I.1** The EPR spectra of irradiated dose at 100, 200, 500, 1000 and 2000 cGy alanine with microwave power values of 1.589 mW. All spectra were collected with modulation amplitude of 7.018 G and sweep time of 40.45 s.

As illustrated in Figure 3.9 (red line), the spectrum from the EPR signal was being observed until a clear spectrum was seen. The optimal MP was being recorded for each dose at this point. Finally, the MP square of all doses against the EPR intensity graph was plotted. However, in this figure shows the EPR response changes linearly with the square root of MP at the beginning and then deviates from this linearity.

Therefore, to obtain better sensitivity and good reproducibility MP and MA were determined from the highest limit of the linear part of Figure II.2 and Figure II.3
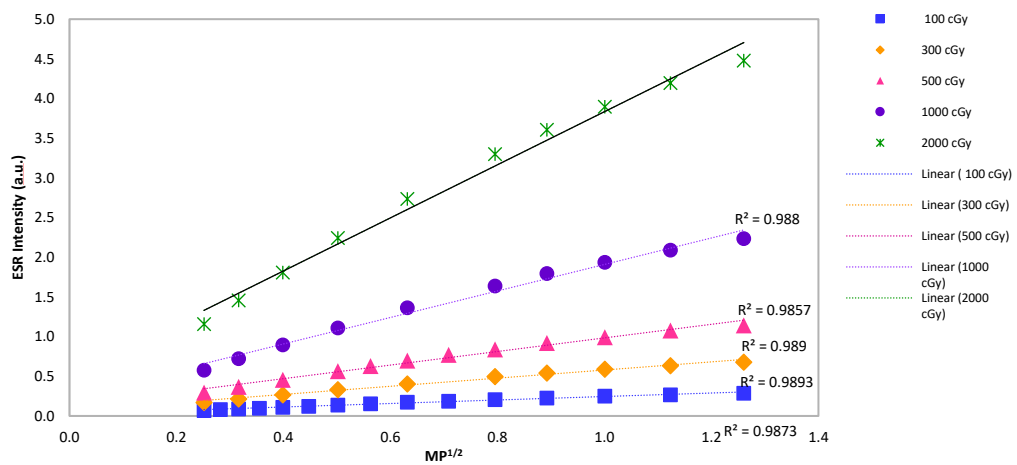


**Figure I.2** The MP square of all doses was plotted against the EPR intensity graph. the highest limit of the linear part at $MP^{1/2} = 1.26$ (MP = 1.589 mW)
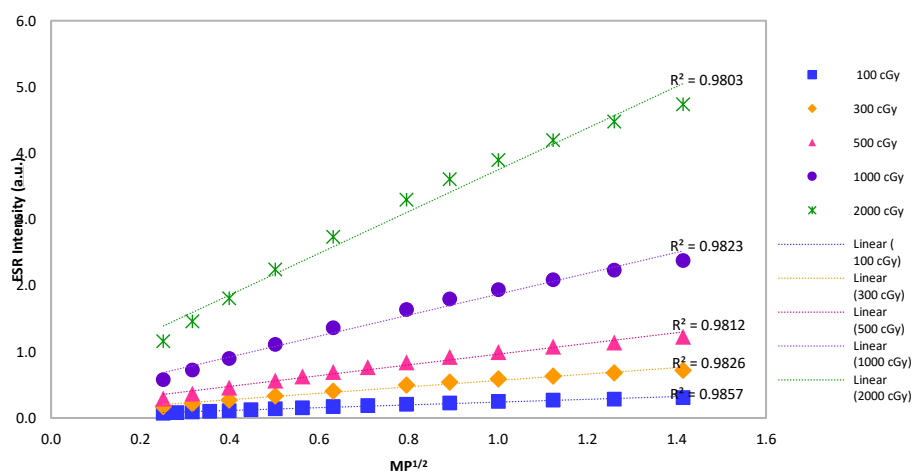


**Figure I.3** The MP square of all doses was plotted against the EPR intensity graph. The highest limit of the linear part at $MP^{1/2} = 1.41$ (MP = 2.000 mW)

**Modulation amplitude (MA)** was used as the acquisition parameter following the preceding. The optimal MP obtained in the first measurement of MP was used as a fixed parameter, and TC was set to a minimum of 0.01 msec. MA was adjusted at 1.000, 2.000, 2.999, 4.000, 5.000, 6.006, 6.579, 7.018, 7.576, 8.032, 8.584, 9.050, 9.569, and 10.050 G (this is a fixed MA step of the EPR machine which user cannot alter) at doses 100, 300, 500, 1000, and 2000 cGy as shown in Table I.2.

**Table I.2** The results of microwave power (MP) fixed at MP=1.589 mW, while MA was attenuated one step from 1 to 10 G and all other parameters were adjusted as described above.

| MA (G) | EPR Intensity (a.u) | | | | |
|---|---|---|---|---|---|
| | 100 cGy | 300 cGy | 500 cGy | 1000 cGy | 2000 cGy |
| 1.000 | 0.0605 | 0.1306 | 0.2089 | 0.4099 | 0.8247 |
| 2.000 | 0.1008 | 0.2465 | 0.3989 | 0.6201 | 1.5703 |
| 2.999 | 0.1491 | 0.3774 | 0.6227 | 0.9344 | 2.3923 |
| 4.000 | 0.1821 | 0.4710 | 0.7824 | 1.1541 | 3.0139 |
| 5.000 | 0.2196 | 0.5577 | 0.9251 | 1.3431 | 3.5760 |
| 6.006 | 0.2478 | 0.6370 | 1.0583 | 1.5066 | 4.0750 |
| 6.579 | 0.2689 | 0.6812 | 1.1234 | 1.5880 | 4.3331 |
| 7.018 | 0.2803 | 0.7100 | 1.1720 | 1.6425 | 4.5079 |
| 7.576 | 0.2953 | 0.7461 | 1.2220 | 1.7079 | 4.7170 |
| 8.032 | 0.2963 | 0.7689 | 1.2588 | 1.7563 | 4.8575 |
| 8.584 | 0.3102 | 0.7921 | 1.3016 | 1.7986 | 5.0075 |
| 9.050 | 0.3140 | 0.8088 | 1.3267 | 1.8243 | 5.0958 |
| 9.569 | 0.3200 | 0.8238 | 1.3456 | 1.8561 | 5.1940 |
| 10.050 | 0.3205 | 0.8333 | 1.3621 | 1.8661 | 5.2465 |

As illustrated in Figure 3.10 (red line), the spectrum from the EPR signal was being observed until a clear spectrum was seen. The optimal MA was being recorded for each dose at this point. Finally, the MA square of all doses against the EPR intensity graph was plotted. However, in this figure shows the EPR response changes linearly with the MA at the beginning and then deviates from this linearity.

Therefore, to obtain better sensitivity and good reproducibility MP and MA were determined from the highest limit of the linear part of Figure II.4 and Figure II.5
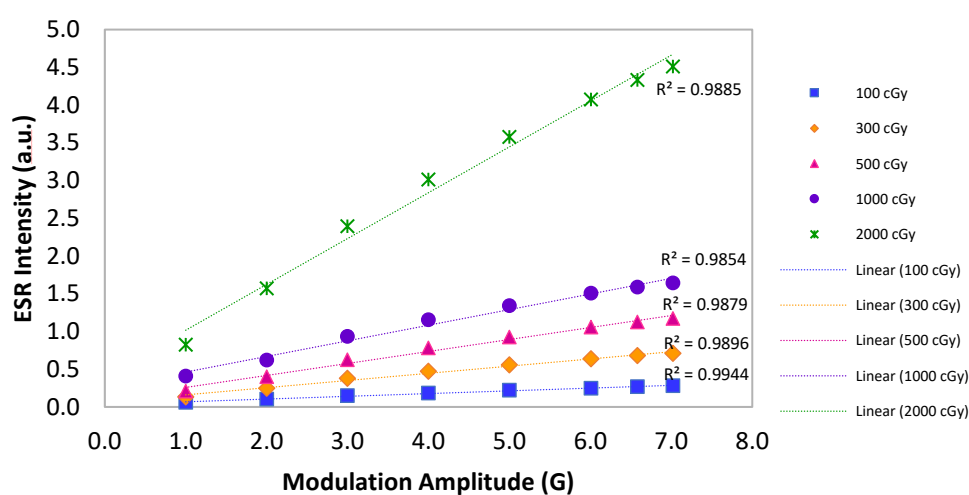


**Figure I.4** The MP square of all doses was plotted against the EPR intensity graph. The highest limit of the linear part at MA = 7.018 G.
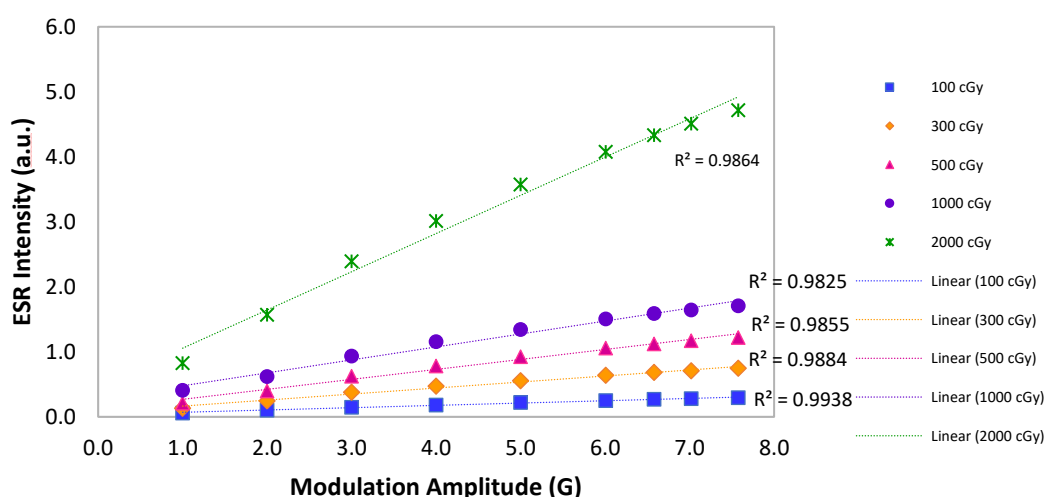


**Figure I.5** The MA of all doses was plotted against the EPR intensity graph. The highest limit of the linear part at MA = 7.575 G.

Time constant (TC), the optimal MP and MA obtained from above procedures were used as fixed parameters to set TC at 0.01, 0.02, 0.04, 0.08, 0.16, 0.32, 0.64, 1.28, 2.56, 5.12, 10.24, 20.48, 40.96, 81.92, 163.84, 327.68, 655.36, 1310.72, 2521.44, and 5242.88 msec (this is a fixed TC step of EPR machine which user cannot adjust). As indicated in Figure I.6 to Figure I.25 in each TC and Figure I.26 shown the graph of TC, the EPR signal was observed, and the peak-to-peak width (**Δ**BPP) was measured. Each **Δ**BPP was normalized to **Δ**BPP of TC 0.01 msec at doses of 1000 cGy.
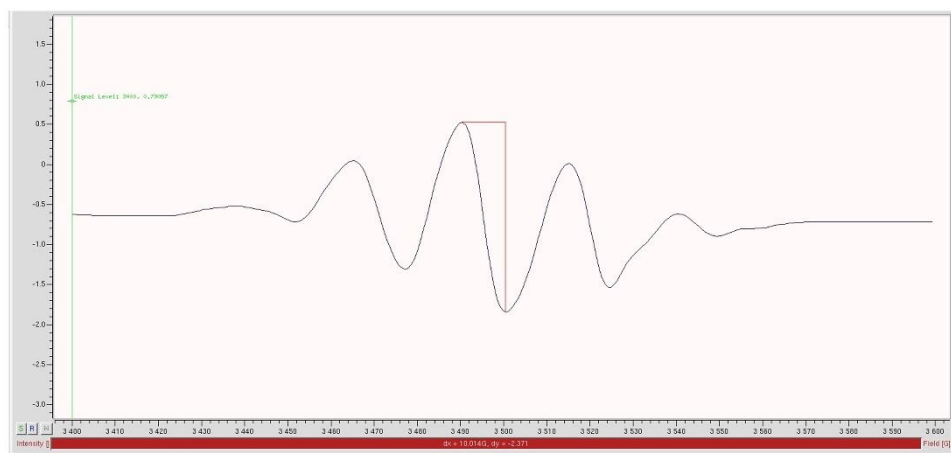


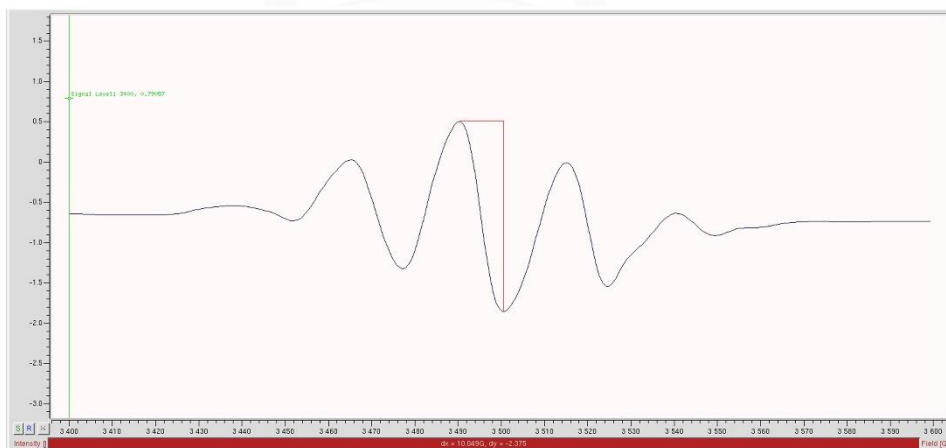**Figure I.6** The peak-to-peak width (**Δ**BPP) was 10.014 G of the TC=0.01 msec at the dose of 1000 cGy



**Figure I.7** The peak-to-peak width (**Δ**BPP) was 10.049 G of the TC=0.02 msec at the dose of 1000 cGy

***Figure  I.8*** *The peak-to-peak width (**Δ**BPP) was 10.049 G of the TC=0.04 msec at the*
*dose of 1000 cGy*



**Figure  I.9** The peak-to-peak width (**Δ**BPP) was 10.049 G of the TC=0.08 msec at the
dose of 1000 cGy



**Figure  I.10** The peak-to-peak width (**Δ**BPP) was 10.049 G of the TC=0.16 msec at the
dose of 1000 cGy

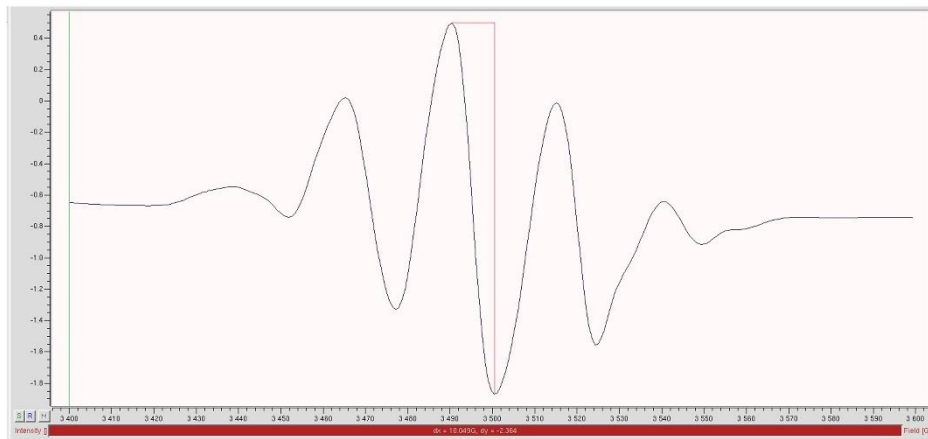**Figure I.11** The peak-to-peak width (**Δ**BPP) was 10.049 G of the TC=0.32 msec at the dose of 1000 cGy



**Figure I.12** The peak-to-peak width (**Δ**BPP) was 10.049 G of the TC=0.64 msec at the dose of 1000 cGy
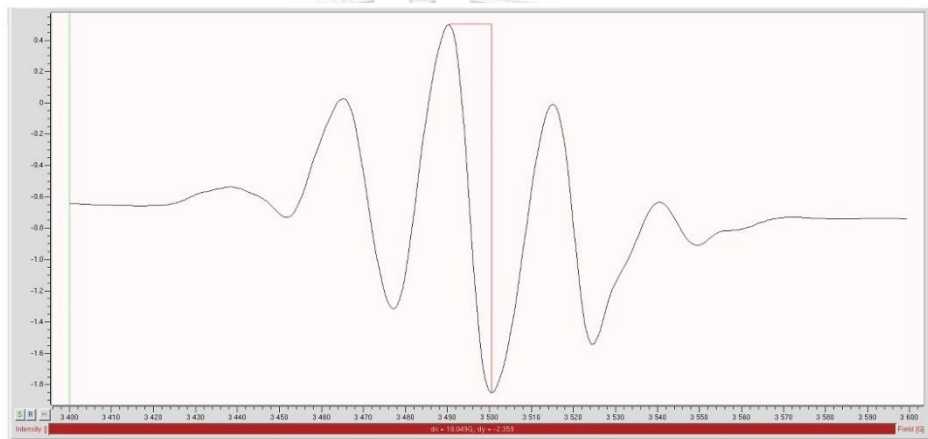


**Figure I.13** The peak-to-peak width (**Δ**BPP) was 10.154 G of the TC=1.28 msec at the dose of 1000 cGy

**Figure  I.14** The peak-to-peak width (**Δ**BPP) was 10.183 G of the TC=2.56 msec at the dose of 1000 cGy
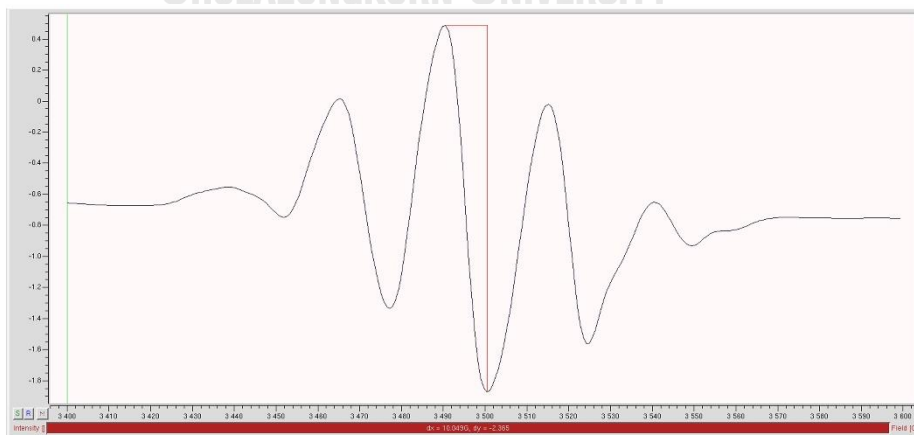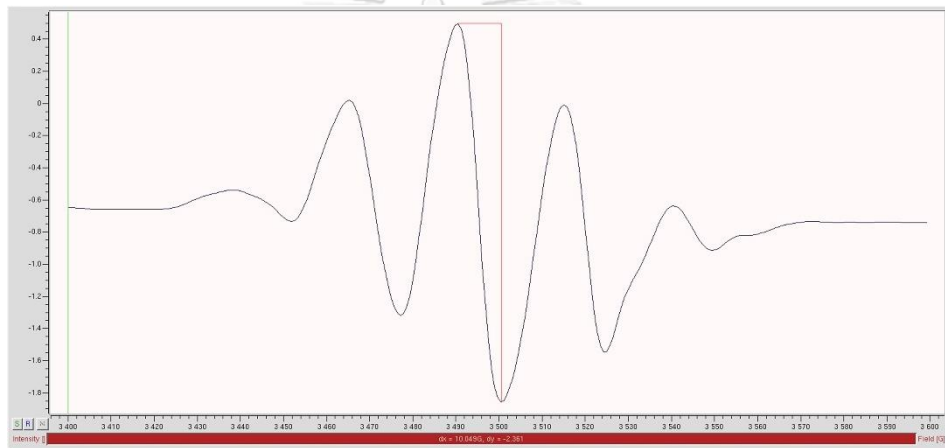


**Figure  I.15** The peak-to-peak width (**Δ**BPP) was 10.049 G of the TC=5.12 msec at the dose of 1000 cGy
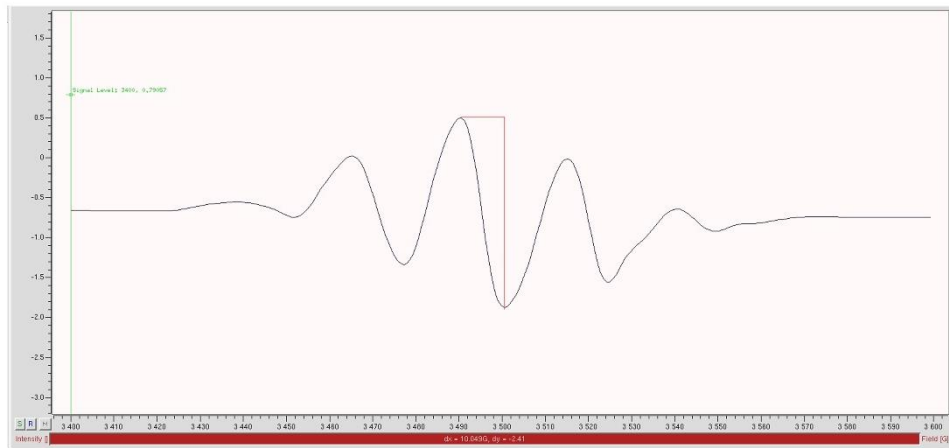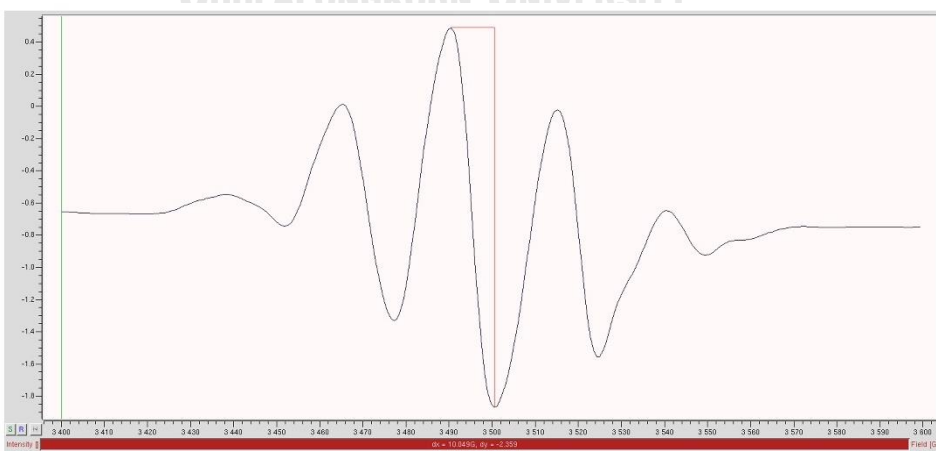


**Figure  I.16** The peak-to-peak width (**Δ**BPP) was 10.049 G of the TC=10.24 msec at the dose of 1000 cGy
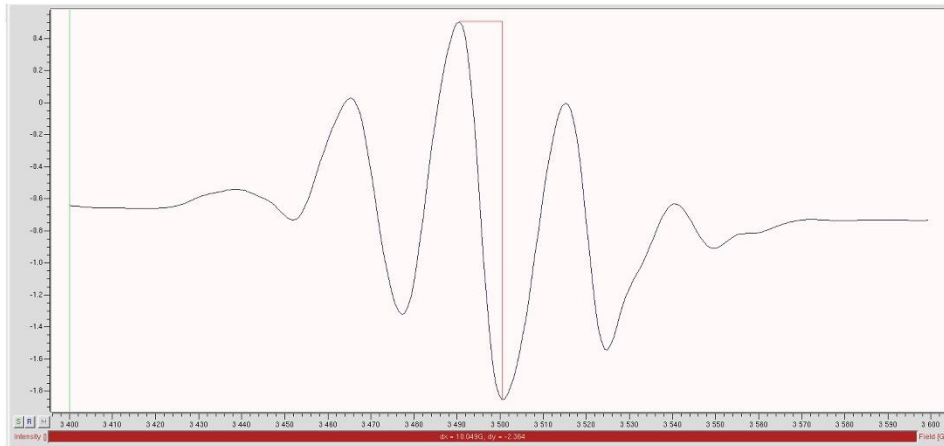
**Figure I.17** The peak-to-peak width (**Δ**BPP) was 10.049 G of the TC=20.48 msec at the dose of 1000 cGy
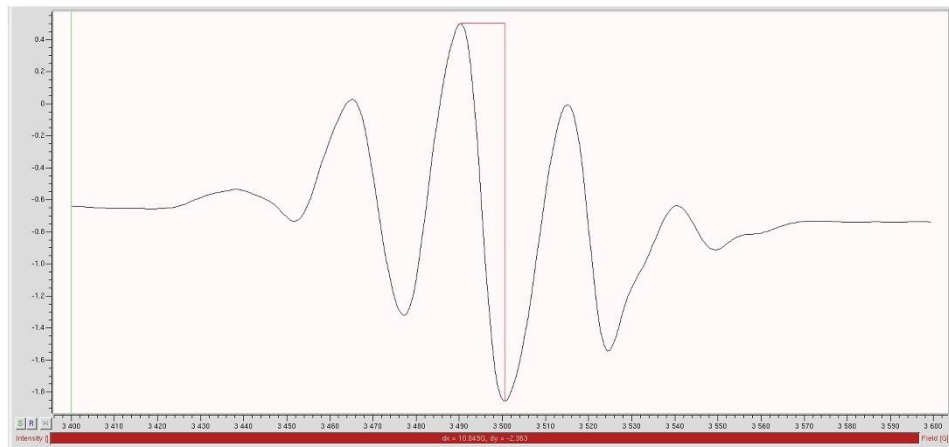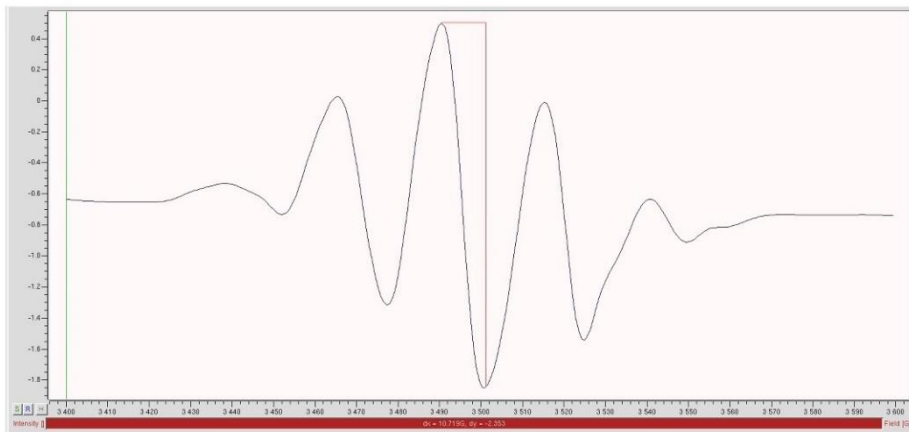


**Figure I.18** The peak-to-peak width (**Δ**BPP) was 10.719 G of the TC=40.96 msec at the dose of 1000 cGy
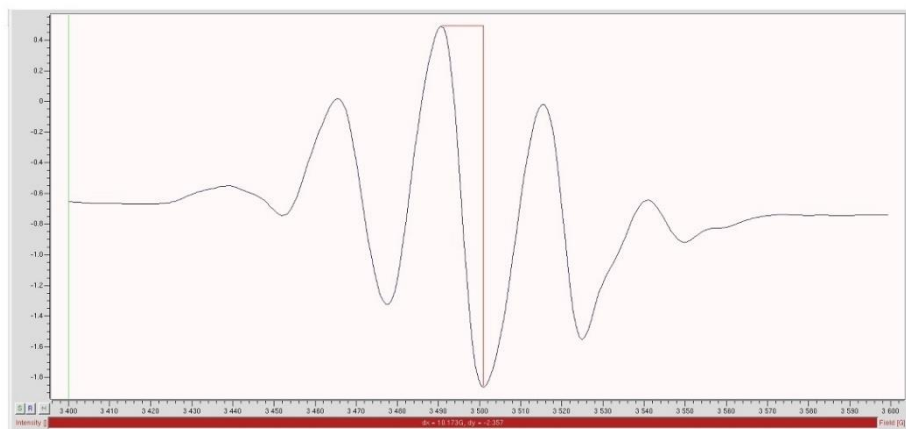


**Figure I.19** The peak-to-peak width (**Δ**BPP) was 10.173 G of the TC=81.92 msec at the dose of 1000 cGy
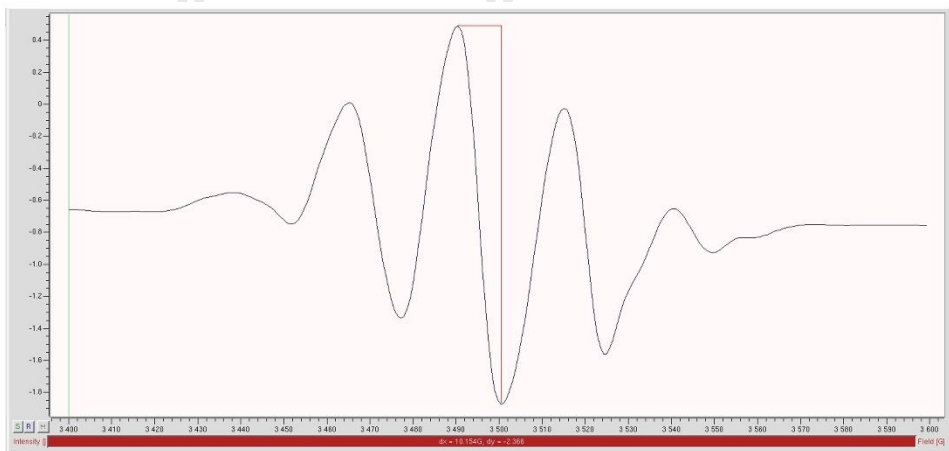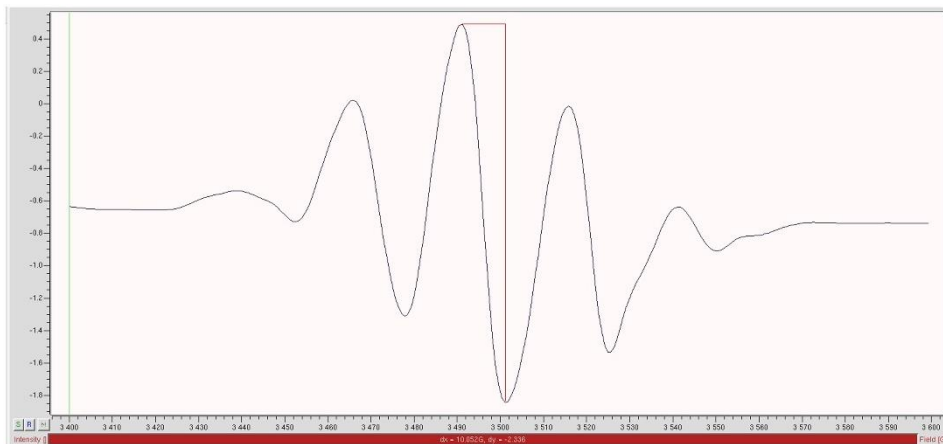
**Figure I.20** The peak-to-peak width (ΔBPP) was 10.052 G of the TC=163.84 msec at the dose of 1000 cGy
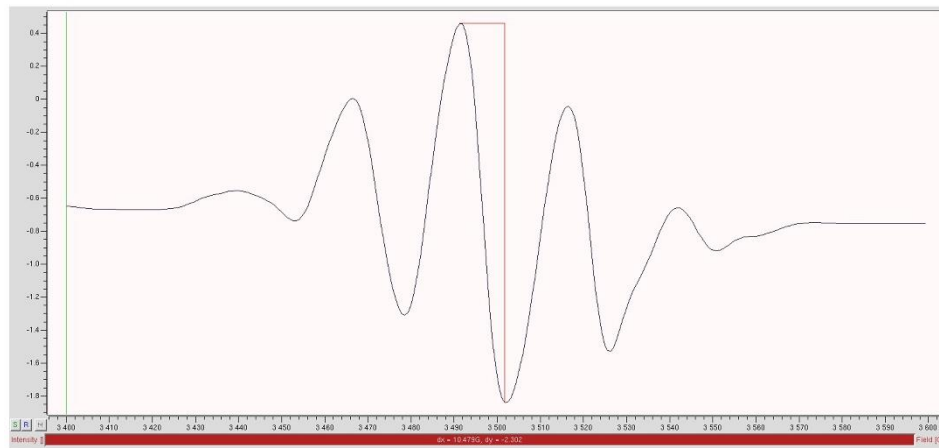


**Figure I.21** The peak-to-peak width (ΔBPP) was 10.479 G of the TC=327.68 msec at the dose of 1000 cGy



**Figure I.22** The peak-to-peak width (ΔBPP) was 11.388 G of the TC=655.36 msec at the dose of 1000 cGy
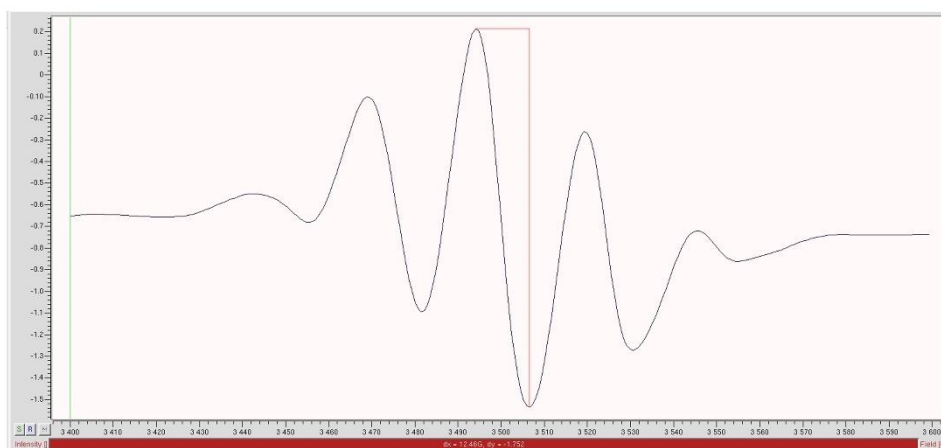
**Figure  0.23** The peak-to-peak width (**Δ**BPP) was 12.460 G of the TC=1310.72 msec at the dose of 1000 cGy
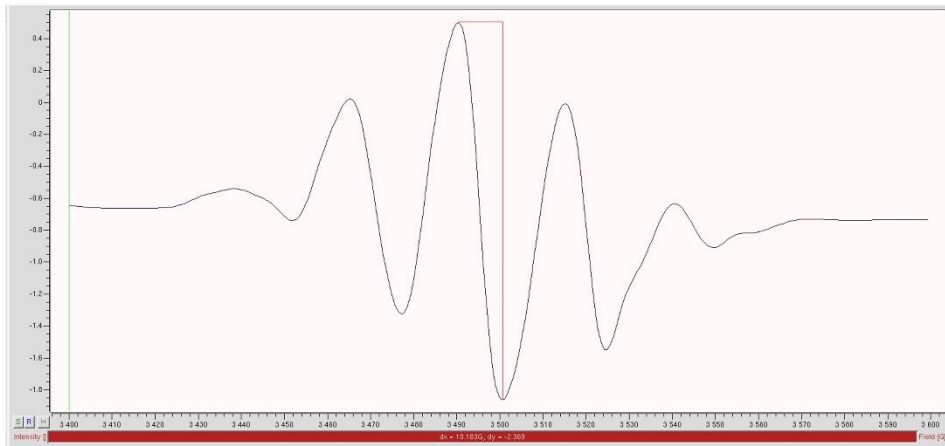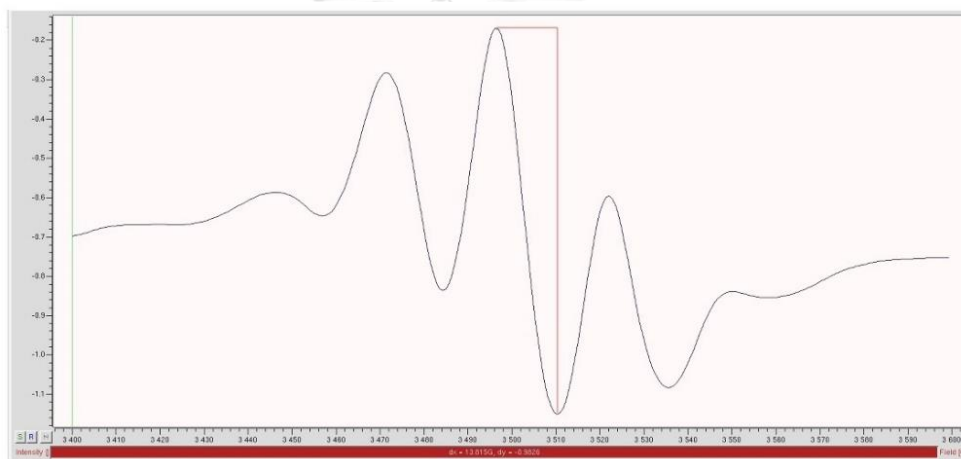


**Figure  0.24** The peak-to-peak width (**Δ**BPP) was 13.815 G of the TC=2521.44 msec at the dose of 1000 cGy
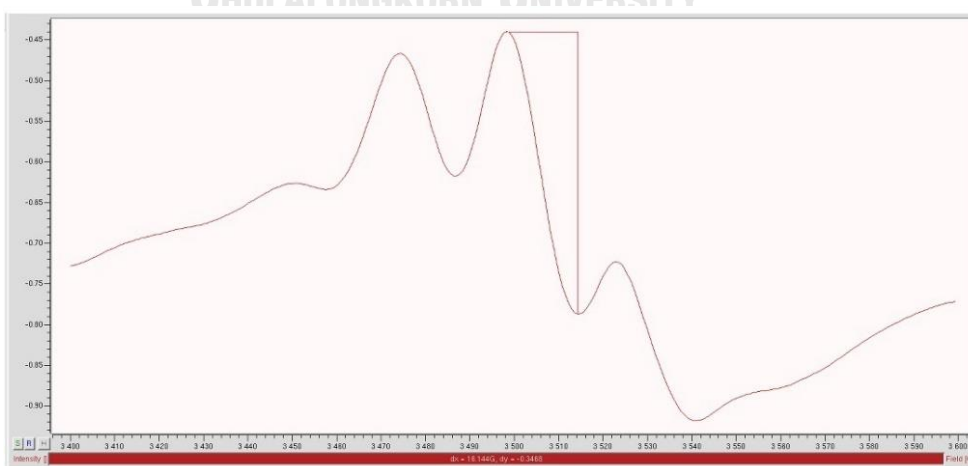


**Figure  I.25** The peak-to-peak width (**Δ**BPP) was 16.144 G of the TC=5242.88 msec at the dose of 1000 cGy
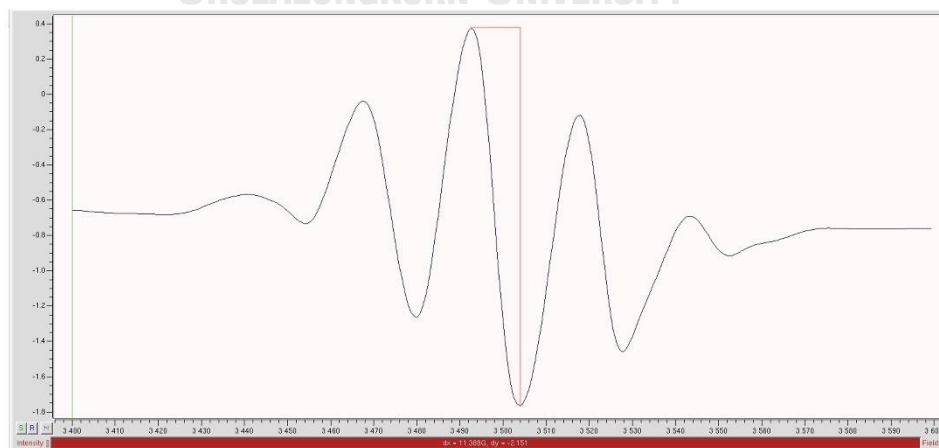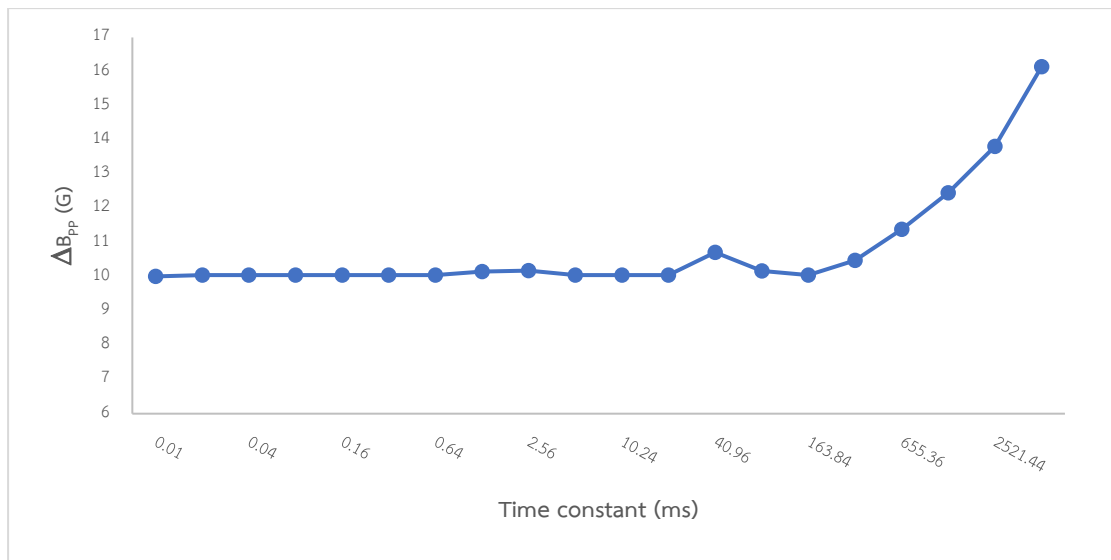
**Figure I.26** The Time constant (TC) at 0.01, 0.02, 0.04, 0.08, 0.16, 0.32, 0.64, 1.28, 2.56, 5.12, 10.24, 20.48, 40.96, 81.92, 163.84, 327.68, 655.36, 1310.72, 2521.44, and 5242.88 msec at the dose of 1000 cGy

## APPENDIX II

### Alanine characteristics

**Uniformity and reproducibility**

Ten alanine pellets were irradiated at the same time with 1000 cGy at 6 MV-FFF, 100 cm SSD, with a field size of 10 x 10 cm$^2$ at 1.5 cm depth. EPR intensity was read at each alanine pellet. The uniformity of the alanine dosimeter from 10 alanine pellets is presented in Tabel II.1. The relative response of each alanine pellet was normalized to the average EPR intensity of 10 alanine which were measured 3 measurements. The reproducibility was determined by the average EPR intensity of five times readout for each alanine pellet which is shown in Tabel II.2.

**Table II.1** Uniformity of 10 alanine for 6MV-FFF was performed three measurements. The readout of alanine dosimeters was normalized to the average of 10 alanine dosimeters.

| Number | EPR Intensity (a.u.) | | | Mean | SD | %CV | Relative EPR |
| of pellet | Rep 1 | Rep 2 | Rep 3 | | | | Intensity |
|---|---|---|---|---|---|---|---|
| 1 | 0.6118 | 0.6138 | 0.6149 | 0.6135 | 0.0016 | 0.26 | 0.984 |
| 2 | 0.6312 | 0.6294 | 0.6283 | 0.6296 | 0.0015 | 0.23 | 1.010 |
| 3 | 0.6311 | 0.6299 | 0.6299 | 0.6303 | 0.0007 | 0.11 | 1.011 |
| 4 | 0.6220 | 0.6211 | 0.6237 | 0.6223 | 0.0013 | 0.21 | 0.998 |
| 5 | 0.6218 | 0.6245 | 0.6228 | 0.6230 | 0.0014 | 0.22 | 1.000 |
| 6 | 0.6285 | 0.6290 | 0.6275 | 0.6283 | 0.0008 | 0.12 | 1.008 |
| 7 | 0.6187 | 0.6189 | 0.6164 | 0.6180 | 0.0014 | 0.22 | 0.992 |
| 8 | 0.6305 | 0.6315 | 0.6284 | 0.6301 | 0.0015 | 0.24 | 1.011 |
| 9 | 0.6228 | 0.6219 | 0.6206 | 0.6218 | 0.0011 | 0.18 | 0.998 |
| 10 | 0.6151 | 0.6167 | 0.6142 | 0.6153 | 0.0037 | 0.60 | 0.987 |
| Mean | 0.6234 | | | 0.6232 | 0.0015 | 0.24 | |
| SD | 0.0065 | | | | | | |
| %CV | 1.05 | | | | | | |

**Table II.2** The reproducibility was determined by the average EPR intensity of five times readout for each alanine pellet

| Number of pellet | EPR Intensity (a.u.) | | | | | Mean | SD | %CV |
|---|---|---|---|---|---|---|---|---|
| | Rep 1 | Rep 2 | Rep 3 | Rep 4 | Rep 5 | | | |
| 1 | 0.6118 | 0.6138 | 0.6149 | 0.6119 | 0.6149 | 0.613 | 0.002 | 0.25 |
| 2 | 0.6312 | 0.6294 | 0.6283 | 0.6307 | 0.6319 | 0.630 | 0.001 | 0.23 |
| 3 | 0.6311 | 0.6299 | 0.6299 | 0.6303 | 0.6274 | 0.630 | 0.001 | 0.23 |
| 4 | 0.6220 | 0.6211 | 0.6237 | 0.6190 | 0.6222 | 0.622 | 0.002 | 0.28 |
| 5 | 0.6218 | 0.6245 | 0.6228 | 0.6211 | 0.6220 | 0.622 | 0.001 | 0.20 |
| 6 | 0.6285 | 0.6290 | 0.6275 | 0.6273 | 0.6278 | 0.628 | 0.001 | 0.11 |
| 7 | 0.6187 | 0.6189 | 0.6164 | 0.6207 | 0.6185 | 0.619 | 0.002 | 0.25 |
| 8 | 0.6305 | 0.6315 | 0.6284 | 0.6282 | 0.6296 | 0.630 | 0.001 | 0.22 |
| 9 | 0.6228 | 0.6219 | 0.6206 | 0.6236 | 0.6226 | 0.622 | 0.001 | 0.18 |
| 10 | 0.6151 | 0.6167 | 0.6142 | 0.6139 | 0.6148 | 0.615 | 0.001 | 0.18 |
| Mean | 0.6234 | | | | | 0.623 | 0.001 | 0.21 |
| SD | 0.0065 | | | | | | | |
| %CV | 1.05 | | | | | | | |

**Linearity**

The ten alanine pellets were irradiated in five doses of 0, 200, 500, 1000, 1500, 2000, and 3000 Gy from 6MV-FFF, 100 cm SSD, with a field size of 10 x 10 cm$^2$ at 1.5 cm depth. The increase in dose-response signal value was correlated to the radiation dose as shown in Tabel II.3. The EPR intensity and radiation dose were plotted is presented in Figure 4.4. The response of the alanine dosimeter yielded a linear dose range from 0 to 3000 cGy presented the R$^2$ of 0.9998 and a linear equation obtained is y = 0.000585x + 0.0294, slope in this equation represent the sensitivity was 0.000585 a.u./cGy. For verified the calibration curve the unknow dose was irradiated and calculated the dose (cGy) from a linear equation: y = 0.000585x + 0.0294. Hence the dose was calculated from this equation; Dose = (EPR intensity-0.0294)/0.000585 which the data was presented in Tabel II.4.

**Table II.3** The EPR intensity of 10 alanine linear dose ranges from 0 to 3000 cGy.

| Number | EPR Intensity (a.u.) | | | | | | |
|---|---|---|---|---|---|---|---|
| of pellet | 0 cGy | 200 cGy | 500 cGy | 1000 cGy | 1500 cGy | 2000 cGy | 3000 cGy |
| 1 | 0.0348 | 0.1402 | 0.3129 | 0.6118 | 0.8923 | 1.2385 | 1.7079 |
| 2 | 0.0396 | 0.1423 | 0.3120 | 0.6312 | 0.8982 | 1.2139 | 1.7950 |
| 3 | 0.0397 | 0.1424 | 0.3185 | 0.6311 | 0.9002 | 1.2046 | 1.8042 |
| 4 | 0.0447 | 0.1405 | 0.3164 | 0.6220 | 0.8957 | 1.2015 | 1.7951 |
| 5 | 0.0448 | 0.1394 | 0.3164 | 0.6218 | 0.9011 | 1.1954 | 1.8057 |
| 6 | 0.0295 | 0.1405 | 0.3130 | 0.6285 | 0.9159 | 1.2023 | 1.7697 |
| 7 | 0.0397 | 0.1410 | 0.3141 | 0.6187 | 0.8837 | 1.2048 | 1.7612 |
| 8 | 0.0340 | 0.1420 | 0.3167 | 0.6305 | 0.8851 | 1.1864 | 1.8007 |
| 9 | 0.0433 | 0.1398 | 0.3087 | 0.6228 | 0.9077 | 1.2050 | 1.8139 |
| 10 | 0.0378 | 0.1388 | 0.3127 | 0.6151 | 0.8875 | 1.1931 | 1.7969 |
| Mean | 0.0388 | 0.1407 | 0.3141 | 0.6234 | 0.8967 | 1.2045 | 1.7850 |
| SD | 0.0047 | 0.0012 | 0.0027 | 0.0065 | 0.0097 | 0.0134 | 0.0300 |
| %CV | 12.1 | 0.8 | 0.9 | 1.0 | 1.1 | 1.1 | 1.7 |

**Table II.4** The EPR intensity of 10 alanine from unknow dose. (%Difference = $(D_{calculated} - D_{stated})/D_{stated}*100$).

| Number | EPR Intensity (a.u.) | y = 0.000585x + 0.0294 | % Difference |
|---|---|---|---|
| of pellet | Unknow dose (cGy) | Calculated dose (cGy) | |
| 1 | 0.7261 | 1190.95 | 0.75 |
| 2 | 0.7264 | 1191.46 | 0.71 |
| 3 | 0.7215 | 1183.12 | 1.41 |
| 4 | 0.7317 | 1200.45 | -0.04 |
| 5 | 0.7175 | 1176.25 | 1.98 |
| 6 | 0.7398 | 1214.38 | -1.20 |
| 7 | 0.7214 | 1182.94 | 1.42 |
| 8 | 0.7212 | 1182.62 | 1.45 |
| 9 | 0.7304 | 1198.32 | 0.14 |
| 10 | 0.7325 | 1201.90 | -0.16 |
| Mean | 0.7269 | | |
| SD | 0.0064 | | |
| %CV | 0.9 | | |

**Repetition rate**

        To study the response of alanine against high MU rate, five alanine pellets were irradiated with 10 Gy from 6MV-FFF, 100 cm SSD, with a field size of 10 x 10 $cm^2$ at 1.5 cm depth. The response of alanine dosimeter subjected to a varying repetition rate at 400, 800, 1200, and 1400 MU/min, respectively. Table II.5 shows EPR intensity of five alanine pellets at each repetition rate (MU/min).

**Table II.5** EPR intensity of five alanine pellets at each repetition rate (MU/min)

| Alanine pellets | EPR Intensity (a.u.) | | | |
|:---:|:---:|:---:|:---:|:---:|
| | 400 (MU/min) | 800 (MU/min) | 1200 (MU/min) | 1400 (MU/min) |
| 1 | 0.6395 | 0.6292 | 0.6219 | 0.6336 |
| 2 | 0.6357 | 0.6318 | 0.6301 | 0.6221 |
| 3 | 0.6383 | 0.6277 | 0.6360 | 0.6346 |
| 4 | 0.6256 | 0.6268 | 0.6321 | 0.6318 |
| 5 | 0.6371 | 0.6306 | 0.6239 | 0.6283 |
| Mean | 0.6352 | 0.6292 | 0.6288 | 0.6301 |
| SD | 0.0050 | 0.0018 | 0.0052 | 0.0045 |
| %CV | 0.78 | 0.29 | 0.83 | 0.72 |

**Energy dependence**

        Five alanine pellets were irradiated with 10 Gy, 100 cm SSD, with a field size of 10 x 10 $cm^2$ at 1.5 cm depth from 6MV, 6MV-FFF, as well as at 2.5 cm depth from 10MV, and 10MV-FFF. For 6MV was performed at 600 MU/min, while 6MV-FFF, 10MV, and 10MV-FFF was achieved at 1400 MU/min. Table II.6 shows the result of energy dependence of the alanine dosimeter from varied photon beams.

**Table  II.6** The result of energy dependence of the alanine dosimeter from varied photon beams.

| Alanine pellets | EPR Intensity (a.u.) | | | |
|:---:|:---:|:---:|:---:|:---:|
| | 6MV | 6MV-FFF | 10MV | 10MV-FFF |
| 1 | 0.6297 | 0.6253 | 0.6148 | 0.6329 |
| 2 | 0.6363 | 0.6301 | 0.6203 | 0.6231 |
| 3 | 0.6312 | 0.6286 | 0.6301 | 0.6244 |
| 4 | 0.6289 | 0.6242 | 0.6194 | 0.6248 |
| 5 | 0.6244 | 0.6266 | 0.6244 | 0.6215 |
| Mean | 0.6301 | 0.6269 | 0.6218 | 0.6253 |
| SD | 0.0038 | 0.0021 | 0.0051 | 0.0039 |
| %CV | 0.61 | 0.34 | 0.83 | 0.63 |

**Directional dependence**

The five alanine pellets were irradiated with 10 Gy, 100 cm SSD, with a field size of 10 x 10 cm$^2$ at 1.5 cm depth from 6MV-FFF for directional dependence. This was performed in two directions, perpendicular and parallel, as shown in Table II.7.

**Table  II.7** The result of directional dependence of the alanine dosimeter from two directions.

| Alanine pellets | EPR Intensity (a.u.) | |
|:---:|:---:|:---:|
| | Rep1 | Rep2 |
| 1 | 0.6221 | 0.6268 |
| 2 | 0.6211 | 0.6096 |
| 3 | 0.6238 | 0.6145 |
| 4 | 0.6221 | 0.6157 |
| 5 | 0.6230 | 0.6249 |
| Mean | 0.6224 | 0.6183 |
| SD | 0.0009 | 0.0065 |
| %CV | 0.15 | 1.06 |

APPENDIX III

Validation of the fabricated head phantom

**Phantom uniformity**

This measurement was performed by scanning a set of the fabricated phantom in a CT simulator (GE HealthCare, Chicago, IL, USA) with a slice thickness of 1.25 mm at 120 kV. Next, the CT images were imported in the Eclipse (Varian Medical System Inc, Palo Alto, CA, USA) TPS for uniformity measurement. The ROI were four which is performed CT number in Figure III.1 and the results shown in Tabel III.1.
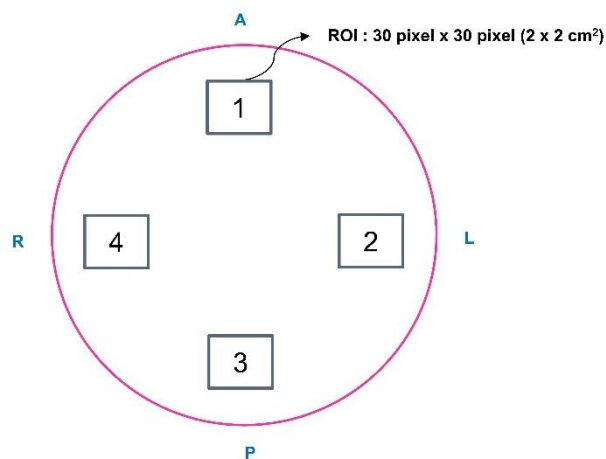


**Figure III.1** The uniformity measurement was scan a set of the fabricated phantom in each ROI.

**Table III.1** The result in each ROI of the fabricated phantom

| ROI Position | CT number (HU) (Mean±SD) |
|:---:|:---:|
| 1 | 90.8±3.72 |
| 2 | 89.8±3.6 |
| 3 | 97.3±4.16 |
| 4 | 91.3±3.72 |

# VITA

| | |
|---|---|
| **NAME** | Aungsumalin Intang |
| **DATE OF BIRTH** | 12 May 1977 |
| **PLACE OF BIRTH** | Phitsanulok, Thailand |
| **INSTITUTIONS ATTENDED** | Naresuan University, 1999 |
| | Bachelor of Science |
| | (Physics) |
| | |
| | Kasetsart University, 2010 |
| | Master of Science |
| | (Applied Radiation and Isotopes) |
| **HOME ADDRESS** | 11/410 P.P.H Condo Soi Chang A-Kad Uthit 11, |
| | Donmuang, Bangkok 10210, Thailand |